Chapter 1. Introduction

Mature blood and immune cells are produced by a network of hierarchically distinct progenitors that arise from hematopoietic stem cells (HSCs) localized within supportive microenvironmental niches in the bone marrow. In order to sustain homeostasis, it is estimated that close to 1 trillion cells are produced each day in a healthy adult male, including 200 billion erythrocytes (red blood cells) and 70 billion polymorphonuclear neutrophils (Ogawa, 1993). This continuous production of blood cells is termed "hematopoiesis" and involves a complex network of cytokines, chemokines, and other growth factors. Maintenance of hematopoiesis involves both intrinsic cues from within individual cells, as well as extrinsic cues from the bone marrow niche. This chapter will provide an overview of the hematopoietic system including the HSC, progenitor cell (HPC), their isolation and function, and hematopoietic regulation by the microenvironment and the bioactive eicosanoid prostaglandin E_2 (PGE_2).

Hematopoiesis and the Hematopoietic Stem Cell

The HSC is an adult stem cell with the unique ability to differentiate down multiple lineages to produce all cells of the blood and immune system, as well as to divide without differentiation in a process termed "self-renewal." The HSC is responsible for lifelong blood production and the continuing replacement of mature erythrocytes; white blood cells such as neutrophils, basophils, eosinophils, dendritic cells, and

macrophages; lymphocytes such as B cells, T-cells, and natural killer (NK) cells; and megakaryocytes that produce platelets.

Clonogenic *in vitro* colony assays and immunophenotypic markers have been used to identify and determine the ability of isolated cells to self-renew and/or differentiate down specific lineages leading to the formation of a hematopoietic hierarchy (Figure 1). Specific progenitor cells have been isolated and characterized including the common lymphoid progenitor (CLP), common myeloid progenitor (CMP), granulocyte-monocyte progenitor (GMP), and the megakaryocyte-erythroid progenitor (MEP) (Kondo *et al.*, 1997; Akashi *et al.*, 2000; Shizuru *et al.*, 2005). These progenitors have been shown to lack the ability to self-renew. Additionally, common myelolymphoid progenitors (CMLP) and common myeloerythroid progenitors (CMEP) have been isolated and suggest that there is not a distinct separation between the myeloid and lymphoid lineages. Multipotent progenitors (MPP), many of which can also be classified as short-term HSCs (ST-HSCs), have also been identified and their limited self-renewal capacity has been demonstrated (Carow *et al.*, 1991; Morrison and Weissman, 1994; Christensen and Weissman, 2001; Yang *et al.* 2005). ST-HSCs are functionally distinct from long-term HSCs (LT-HSCs), which have life-long self-renewal capabilities and have the ability to fully reconstitute life-long hematopoiesis in lethally myeloablated recipients.

Since the LT-HSC is unique in its ability to fully reconstitute hematopoiesis, the only way to definitively demonstrate the presence of a LT-HSC is by transplantation into a lethally irradiated host. Given enough time, the LT-HSC will functionally restore normal

hematopoiesis (Harrison, 1972). However, serial transplantation studies have revealed decreasing self-renewal capabilities of donor cells (Vos, 1972; Vos and Dolmans, 1972) leading to the characterization of HSCs capable of reconstituting hematopoiesis into phenotypically distinct populations. ST-HSCs possess full reconstitution capabilities up to 16 weeks, intermediate-term HSCs (IT-HSCs) are able to reconstitute a host for up to 32 weeks, and LT-HSCs fully reconstitute hematopoiesis for over 32 weeks (Benveniste *et al.*, 2010). The discovery of these distinct populations highlights the need for secondary, or even tertiary, transplant experiments in order to determine long-term reconstitution ability.

Although transplantation and analysis of hematopoietic reconstitution is the only way to definitively determine the presence of a LT-HSC, isolation and characterization of hematopoietic stem and progenitor cell (HSPC) populations has been ongoing since the 1960s. *In vitro* progenitor cell assays, or colony-forming unit (CFU) assays, are used as a measure of the clonogenic potential of cells isolated from the bone marrow or blood. Cells are plated in a semi-solid growth medium and, depending on the presence or absence of specific growth factors, induced to differentiate and produce "colonies" of specific cell types. These colonies have been identified as CFU-granulocyte/macrophage (CFU-GM) (Bradley and Metcalf, 1966; Ichikawa *et al.* 1966; Pluznik and Sachs, 1966), burst-forming erythroid (BFU-E) (Iscove and Sieber, 1975), and mixed colonies of CFU-granulocyte/erythroid/macrophage/monocyte (CFU-GEMM) (Fauser and Messner, 1978; Fauser and Messner, 1979). Based on these assays, the functional capabilities of specific populations of cells can be quantified.

In vitro colony assays were the first to allow for functional characterization of HSPC populations, whereas the advent of fluorescence-activated cell sorting (FACS) has allowed for their phenotypic characterization and enrichment. In 1986, Muller-Sieburg *et al.* identified a population of cells that lacked mature blood cell markers for erythrocytes, neutrophils, macrophages, NK cells, T-cells, and B-cells; this population was termed Lineage$^-$, or Lin$^-$, and found to be enriched for HSPC. Soon after, it was determined that murine Lin$^-$ cells could be further enriched for HSPC by the presence of cell surface markers for stem cell antigen-1 (Sca-1) (Spangrude *et al.*, 1988) and stem cell factor (SCF) receptor (c-kit) (Ogawa *et al*, 1991; Ikuta and Weissman, 1992; Okada *et al.*, 1992). This population of Lin$^-$, Sca-1$^+$, c-kit$^+$ cells is widely accepted to contain HSPC and is referred to as LSK cells.

Although the HSC is found within the LSK population, this group of cells is still heterogeneous and contains numerous types of progenitor cells. Additional markers such as CD34 (Osawa *et al.*, 1996) and *fms*-related tyrosine kinase-3 (Flt3) (Adolfsson *et al.*, 2001; Yang *et al.*, 2005) have been identified within the past 10-20 years that allow for further characterization of the HSPC populations into MPPs (CD34$^+$, Flt3$^+$, LSK), ST-HSCs (CD34$^+$, Flt3$^-$, LSK), and LT-HSC (CD34$^-$, Flt3$^-$, LSK). More recently, the signaling lymphocytic activation molecule (SLAM) markers, which include CD150 and CD48, along with LSK markers were determined to define a highly enriched LT-HSC population (Yimaz *et al.*, 2005; Chen *et al*., 2008). This CD150$^+$, CD48$^-$, LSK population is referred to as SLAM-LSK.

Figure 1

Murine Phenotypic Characterization

Cell	Phenotype
LT-HSC	Lin^- c-kit^+ $Sca1^+$ $Flk2^-$ $CD150^+CD48^-CD34^-CD49b^{lo}$
ST-HSC	Lin^- c-kit^+ $Sca1^+$ $Flk2^-$ $CD150^+$ $CD34^+CD49b^{hi}$
MPP	Lin^- c-kit^+ $Sca1^+$ $Flk2^+$ $CD150^-$ $CD34^+$ $CD49b^{hi}$
CLP	Lin^- c-kit^{lo} $Sca1^{lo}$ $Flk2^{hi}$ IL7Rα$^+$
CMP	Lin^- c-kit^+ $Sca1^-$ $CD34^+$ FcγR^{lo}
GMP	Lin^- c-kit^+ $Sca1^-$ $CD34^-$ FcγR$^+$
MEP	Lin^- c-kit^+ $Sca1^-$ $CD34^-$ FcγR$^-$

Human Phenotypic Characterization

Cell	Phenotype
LT-HSC	Lin^- $CD34^+$ $CD38^-$ $CD90^+$ $CD45RA^-CD49f^+$
MPP	Lin^- $CD34^+$ $CD38^-$ $CD90^-$ $CD45RA^-$ $CD49f^-$
CLP	Lin^- $CD34^+$ $CD38^+$ $CD10^+$
CMP	Lin^- $CD34^+$ $CD38^+$ IL3Rα^{lo} $CD45RA^-$
GMP	Lin^- $CD34^+$ $CD38^+$ IL3Rα$^+$ $CD45RA^-$
MEP	Lin^- $CD34^+$ $CD38^+$ IL3Rα$^-$ $CD45RA^-$

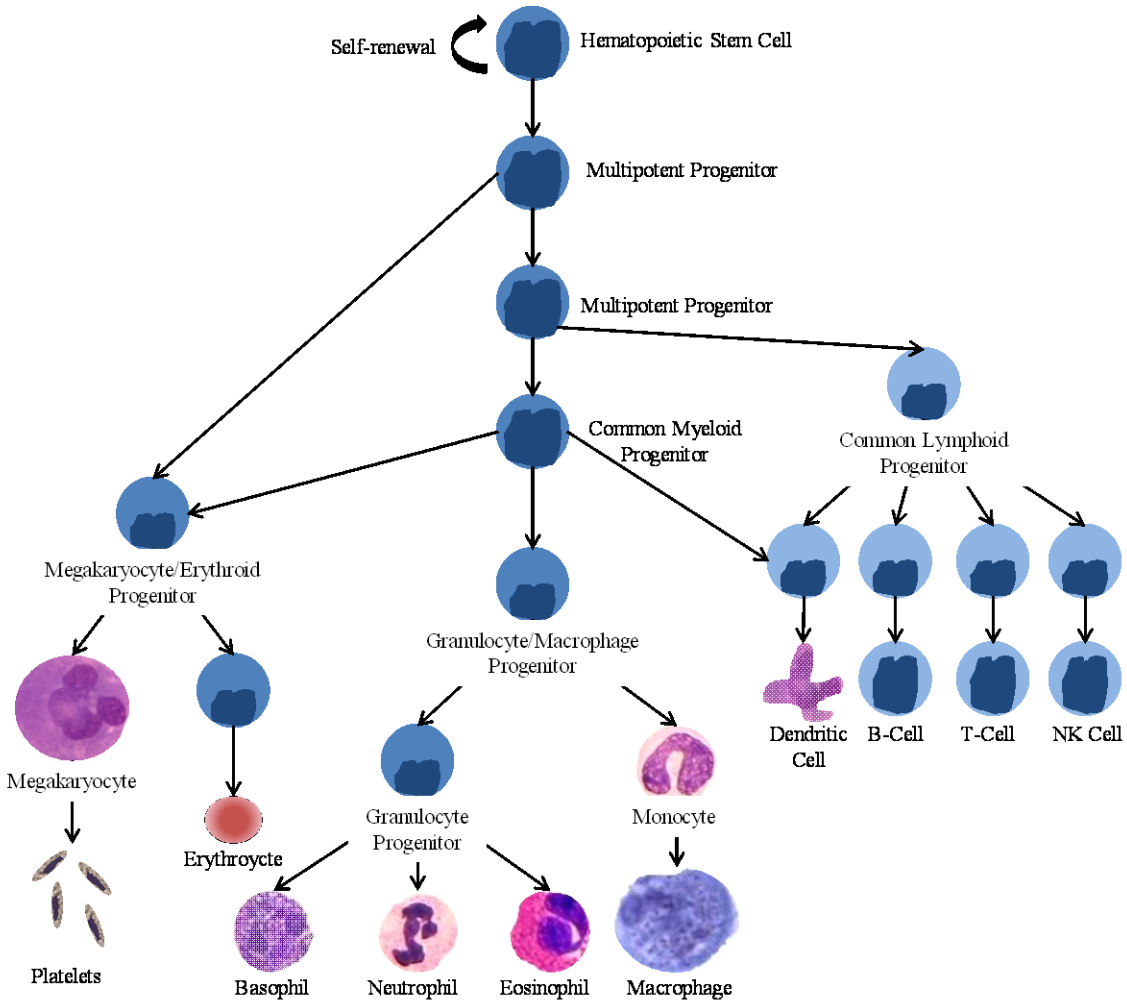

Figure 1. Hematopoietic Hierarchy

Shown is a graphical representation of the hematopoietic stem cell hierarchy based on current understanding of hematopoiesis. Starting at the top, the long-term hematopoietic stem cell is capable of dividing to self-renew and/or to differentiate into multipotent progenitor cells. The MPP cell has limited self-renewal capabilities but is capable of differentiating down multiple lineages. Division of this MPP can produce lineage restricted progenitors including the common myeloid progenitor, common lymphoid progenitor, or megakaryocyte/erythroid progenitor. These progenitors undergo subsequent differentiation steps to produce mature blood cells and platelets.

The Hematopoietic Stem Cell Niche

Maintenance of hematopoiesis at homeostatic levels occurs through regulation of HSPC proliferation, differentiation, and apoptosis via cell intrinsic and extrinsic environmental cues. Blood cells can be found throughout the body, and HSCs may even exit into circulation, but it was first suggested in 1978 that HSCs are maintained in highly specific microenvironments or "niches" within the bone marrow (Schofield, 1978). The bone marrow itself is comprised of mesenchymal stromal cells and extracellular matrix proteins (ECM) including fibronectin, collagen, laminin, and proteoglycans (Yoder and Williams, 1995). Mesenchymal stem cells (MSCs) are a population of cells that, like HSCs, have the ability to self-renew as well as to differentiate down multiple lineages. MSCs differentiate into cells that produce bone (osteoblasts and osteocytes), muscle (myoblasts), cartilage (chondrocytes), and fat (adipocytes) (Bruder *et al.*, 1994; Prockop, 1997). Studies have shown that in a healthy adult skeleton, the rate of bone formation equals the rate of bone loss (Tran Van *et al.*, 1982). At rest, the endosteum of bone is lined with a layer of osteoblasts (OBs). Activation of the osteoclast (bone-resorbing cell) induces a stage of bone resorption, followed by recruitment and differentiation of OB precursors. Osteoblasts deposit an ECM, composed of many different proteins including type I collagen and osteocalcin, within the cavity of resorbed bone that is subsequently mineralized. During this process, some OBs become trapped within the ECM and eventually differentiate into osteocytes (mature bone cells). Following mineralization, OBs become quiescent and again form a single layer along the endosteum (Macdonald and Gowen, 1993).

Since the first suggestion of a hematopoietic stem cell niche, ongoing research strived to discover, characterize, and define components or elements of the bone marrow niche. HSCs within the bone marrow have been shown to have proximal interaction with OBs (Calvi *et al.*, 2003; Arai *et al.*, 2004; Visnjic *et al.*, 2004) leading to the hypothesis of an "endosteal niche" wherein stem cells reside. Co-transplant studies with OBs and/or osteoblast lineage cells have been shown to increase HSC engraftment (El-Badri *et al*., 1998), suggesting that the presence of osteoblast lineage cells are critical for HSC function. Additionally, HSCs have been shown to actively migrate toward and reside within the endosteal region at the interface between bone and bone marrow (Nilsson *et al.*, 1997; Nilsson *et al*, 2001). Osteoblasts lining the endosteum have been shown to both stimulate the expansion of HSCs via a parathyroid-hormone (PTH)-dependent mechanism (Taichman and Emerson, 1994; Taichman *et al*., 2000) and inhibit HSPC proliferation via Osteopontin (OPN) (Nilsson *et al.*, 2005; Stier *et al.*2005) suggesting that OBs are a key regulator of HSPC maintenance and function.

Osteocytes, the most mature osteoblast lineage cell, are found embedded within the bone itself, and have recently been shown to play their own important role in maintenance of hematopoiesis and HSC retention (Bonewald, 2011). Osteocytes release factors such as nitric oxide (NO) and prostaglandins (Klein-Nulend *et al*., 1995), which support osteoblasts. Additionally, the absence of osteocytes causes impaired mobilization of HSCs in response to granulocyte-colony stimulating factor (G-CSF) (Asada *et al.* 2011), suggesting that osteocytes play an important role in HSC trafficking from the bone marrow.

In addition to their association with the endosteal layer of bone, HSCs have also been shown to associate with the sinusoidal endothelium present within the bone marrow (Kiel *et al.*, 2005). The loss of these sinusoidal endothelial cells impairs HSC engraftment in an irradiated recipient (Butler *et al.*, 2010; Hooper *et al.*, 2011), suggesting the likelihood of a "vascular niche." Further experiments suggest that markers expressed on endothelial cells, such as E-selectin, play a crucial role in regulation of HSPC proliferation (Winkler *et al.*, 2012). More recent studies have revealed a role for perivascular stromal cells in HSC maintenance, suggesting the possible presence of a non-endothelial "perivascular niche" (Ding *et al.*, 2012; Corselli *et al.*, 2013). Additionally, Nestin$^+$ MSCs have been implicated as important players in HSC maintenance and retention (Méndez-Ferrer *et al.*, 2010). These Nestin$^+$ PDGFRα$^+$ CD51$^+$ MSCs are spatially associated with HSCs and express important HSC maintenance genes, such as SDF-1, which are downregulated during HSC mobilization (Méndez-Ferrer *et al.*, 2010; Frenette *et al.*, 2013; Pinho *et al*., 2013).

The presence and specific function of distinct bone marrow niches remains a subject of continuous debate, but it is known that HSCs have the ability to interact with cells from all three niches through a number of different adhesion molecules (Kraus *et al*., 2013; Nakamura-Ishizu and Suda, 2013.) (Figure 2). However, one interaction that has been considered to be critically important for regulation of HSPC maintenance and trafficking is CXC chemokine receptor 4 (CXCR4) expressed by HSCs, which binds to stromal-cell derived factor-1 (SDF-1) produced by bone marrow osteoblasts (Ponomaryov *et al.*, 2000), endothelial cells, perivascular cells (Katyama *et al.*, 2006),

and reticular cells (Sugiyama *et al.*, 2006). This central interaction between SDF-1 and CXCR4 has also been shown to have positive effects on HSC proliferation and survival (Zou *et al*., 1998; Broxmeyer *et al.* 2003; Broxmeyer *et al.* 2005; Broxmeyer *et al.* 2007).

Figure 2

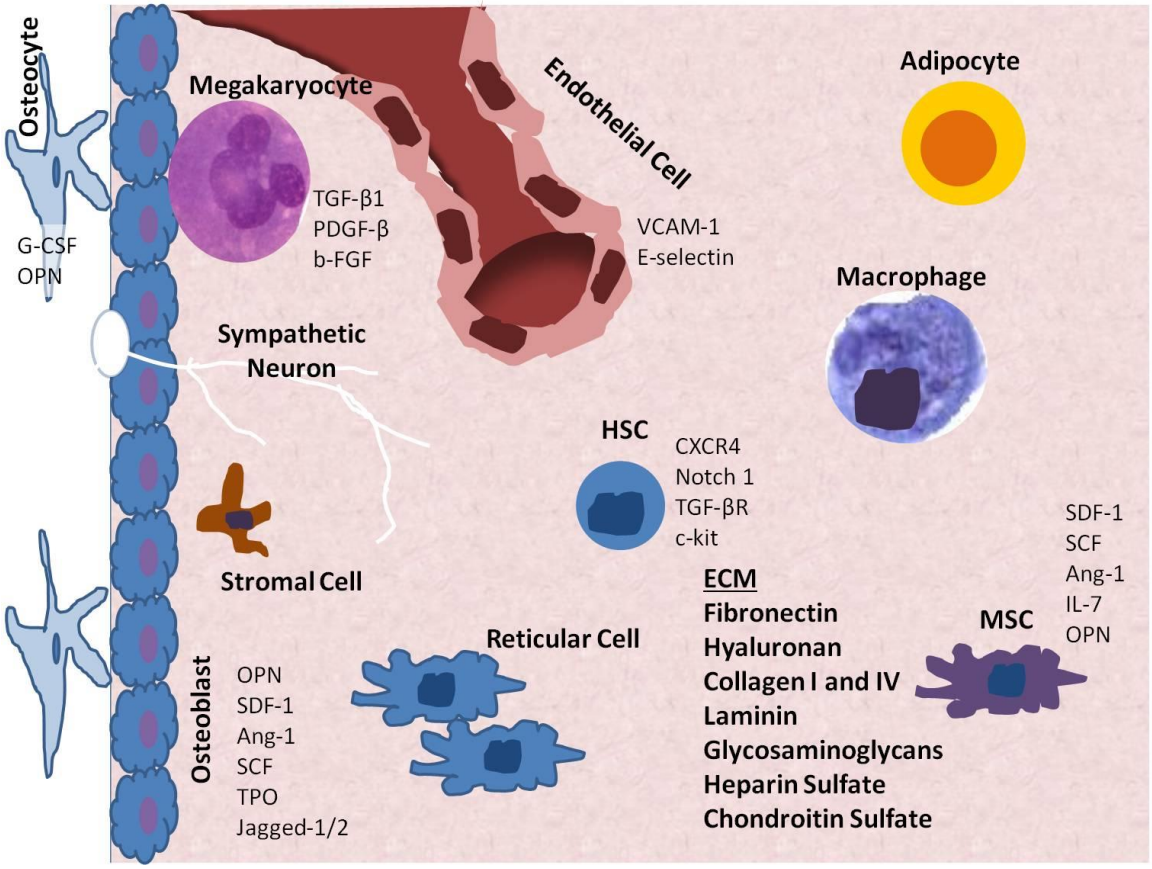
Osteocyte
G-CSF
OPN
Megakaryocyte
TGF-β1
PDGF-β
b-FGF
Endothelial Cell
VCAM-1
E-selectin
Adipocyte
Macrophage
Sympathetic Neuron
HSC
CXCR4
Notch 1
TGF-βR
c-kit
Stromal Cell
ECM
Fibronectin
Hyaluronan
Collagen I and IV
Laminin
Glycosaminoglycans
Heparin Sulfate
Chondroitin Sulfate
MSC
SDF-1
SCF
Ang-1
IL-7
OPN
Reticular Cell
Osteoblast
OPN
SDF-1
Ang-1
SCF
TPO
Jagged-1/2

Figure 2. The Hematopoietic Stem Cell Niche

Shown is an illustration of the proposed components of the hematopoietic stem cell niche within the bone marrow, including both the endosteal and vascular niches. Adhesion molecules, cytokines, chemokines, and growth factors, such as G-CSF, SDF-1, SCF, CXCR4, and OPN, which are important for HSC maintenance and regulation, are also included.

The Megakaryocyte- A Valuable Player in Niche Restoration

Megakaryocytes (MK) are the largest cell present in the bone marrow and one of the rarest. Their most well-known function is the production of platelets, which plays an important role in wound healing, angiogenesis, inflammation, and immunity. MKs develop in the bone marrow from HSCs, directed by the growth factor thrombopoietin (TPO) and its MK-specific receptor c-Mpl (Bartley *et al.*, 1994; de Sauvage *et al.*, 1994; Kaushansky, 1994; Kaushansky *et al.*, 1994; Kuter *et al.*, 1994; Lok *et al.*, 1994; Sohma *et al.*, 1994; Wendling *et al.*, 1994). Driven by TPO, MKs undergo a process called endomitosis in which they become polyploid through cycles of DNA replication without cell division (Ebbe, 1976; Gurney *et al*., 1994) and accumulate a DNA content of 4n-128n in a single nucleus before undergoing final maturation and proplatelet formation (Zimmet and Ravid, 2000). Under normal physiological conditions, MKs are found throughout the bone marrow where they are inhibited from the formation of proplatelets by the presence of collagen I (Sabri *et al.*, 2004; Sabri *et al.*, 2006; Zou *et al.*, 2009). Polyploid MKs then migrate to the bone marrow sinusoid where they form proplatelets, long branching processes that extend through the endothelium and release platelets into the vascular space of the sinusoidal blood vessels of the bone marrow (Tavassoli and Aoki, 1989; Machlus and Italiano, 2013). More recent evidence suggests that up-regulation of SDF-1 and its receptor CXCR4 may play an important role in MK migration to the endothelium (Avecilla *et al.*, 2004; Pitchford *et al.*, 2012).

In addition to the production of platelets, MKs have also been shown to play an important role in the stimulation of OB proliferation and are involved in niche

restoration after bone marrow radioablation. It has been reported that mice deficient in GATA-1 or NF-E2, transcription factors required for MK differentiation, have a marked increase in bone volume (Kacena *et al.*, 2004; Kacena *et al.*, 2006), as well as increased numbers of immature MKs that can interact with OBs causing increased OB proliferation and increased bone mass. The effect of MKs on OB proliferation was determined to be contact-mediated and did not occur when OB were cultured with MK conditioned media or separated from MKs by an impermeable membrane. Extensions of these studies determined that increasing numbers of MKs induce increased OB proliferation, as well as inhibition of osteoclasts (Ciovacco *et al.*, 2010). When MKs were separated into three subpopulations based on maturity, megakaryoblasts ($CD61^+$, $CD41^-$), immature MKs ($CD41^+$, $CD49d^+$), and mature MKs ($CD41^+$, $CD49b^+$), mature and immature MKs were able to stimulate OB proliferation and inhibit osteoclasts, while megakaryoblasts had no effect on either OBs or osteoclasts. Based on these studies, MKs have been defined as Lin^- $CD41^+$ cells for the purpose of this thesis, which includes both mature and immature MKs capable of OB stimulation.

Prior to the discovery that MKs can stimulate OB proliferation, studies demonstrated that the MK growth factor TPO could be used as a radiomitigating agent. Administration of TPO to lethally irradiated mice accelerated recovery of HSPC populations and increased survival up to 90 percent (Mouthon *et al.*, 1999; Mouthon *et al.*, 2002). More recently, a two-fold increase in MKs in close proximity to the endosteal surface was observed at 48 hours after total-body irradiation (TBI), which was associated with increases in SDF-1 and levels of the MK-derived factors platelet-derived

growth factor-β (PDFG-β) and basic fibroblast growth factor (bFGF) (Dominici *et al.*, 2009). This TBI-induced migration of MKs to the endosteum appears to be dependent on TPO signaling through c-Mpl and CD41-mediated adhesion (Olson *et al.*, 2013). These studies suggest that MKs are not only important for platelet production but also play a role in repair of the HSC niche, via stimulation of OB proliferation, particularly after irradiation. The colocalization of MKs and OBs is required for efficient donor cell engraftment following hematopoietic transplantation, at least in mice (Dominici *et al.*, 2009).

Prostaglandins: Synthesis and Signaling

Eicosanoids, such as PGE_2, are a large family of bioactive lipids that are formed by the oxidation of arachidonic acid (AA). PGE_2 is the most abundant eicosanoid molecule (Serhan and Levy, 2003; Murakami and Kudo, 2006) and is known to be a potent mediator of inflammation (Hinson *et al.*, 1996; Murakami and Kudo, 2006; Samuelsson *et al.*, 2007), pain (Schweizer *et al.*, 1988; Stock *et al.*, 2001), fever (Coceani *et al.*, 1989; Ivanov and Romanovsky, 2004; Lazarus, 2006), and cancer (Hull *et al.*, 2004; Murakami and Kudo, 2006).

Prostaglandins are synthesized by all nucleated cells (Miller, 2006). Synthesis of PGE_2 (Figure 3) begins when AA is cleaved from a phospholipid by phospholipase A_2, which can be activated by inflammatory agents, growth factors, increased intracellular calcium, and irradiation (Cohen and DeLeo, 1993; Kang-Rotondo *et al.*, 1993; Clark *et al.*, 1995; Evans *et al.*, 2001; Ivanov and Romanovsky, 2004). Arachidonic acid is then

oxidized by cyclooxygenase enzymes COX 1/2 forming the intermediate PGG_2 (Kuehl *et al.*, 1977a; Kuehl *et al.*, 1977b), which is subsequently reduced to PGH_2. PGH_2 is then isomerized to different prostaglandin molecules by specific synthases (Smith *et al.*, 1991; Ivanov and Romanovsky, 2004; Murakami and Kudo, 2004; Miller, 2006; Park *et al.*, 2006). COX 1 is normally constitutively expressed and responsible for basal function, while COX 2 is induced by cytokines and other inflammatory mediators (Murakami and Kudo, 2004; Miller, 2006; Park *et al.*, 2006). Both COX 1and COX 2 are expressed in the bone marrow (Hoggatt *et al.*, 2013).

Following synthesis, PGE_2 exits the cell via passive or active transport. PGE_2 is able to interact with four G-protein coupled receptors (GPCR): EP1-EP4 (Breyer *et al.*, 2001; Tsuboi *et al.*, 2002; Hull *et al.*, 2004; Sugimoto and Narumiya, 2007), which account for the pleiotropic effects of PGE_2 on different cells and systems of the body (Breyer *et al.*, 2001) (Figure 4). The EP1 receptor activates phospholipase C (PLC) causing increases in intracellular calcium levels (Breyer *et al.*, 2001; Tsuboi *et al.*, 2002). Binding of PGE_2 to the EP3 receptor results in inhibition of adenylate cyclase and, subsequently, reduced cyclic adenosine monophosphate (cAMP) signaling (Lazarus, 2006; Sugimoto and Narumiya, 2007). Opposing the EP3 receptor, both EP2 and EP4 receptors lead to activation of cAMP signaling through phosphokinase A (PKA) (Breyer *et al.*, 2001; Tsuboi *et al.*, 2002; Hull *et al.*, 2004; Sugimoto and Narumiya, 2007). Additionally, signaling through EP4 can also activate the phosphoinositide 3-kinase (PI3K) pathway (Fujino *et al.*, 2003; Vo *et al.*, 2013). As a consequence of signaling overlap as well as opposing

effects, the effects of PGE_2 are highly dependent on concentration, timing, and EP receptor expression and availability (Hull *et al.*, 2004).

Figure 3

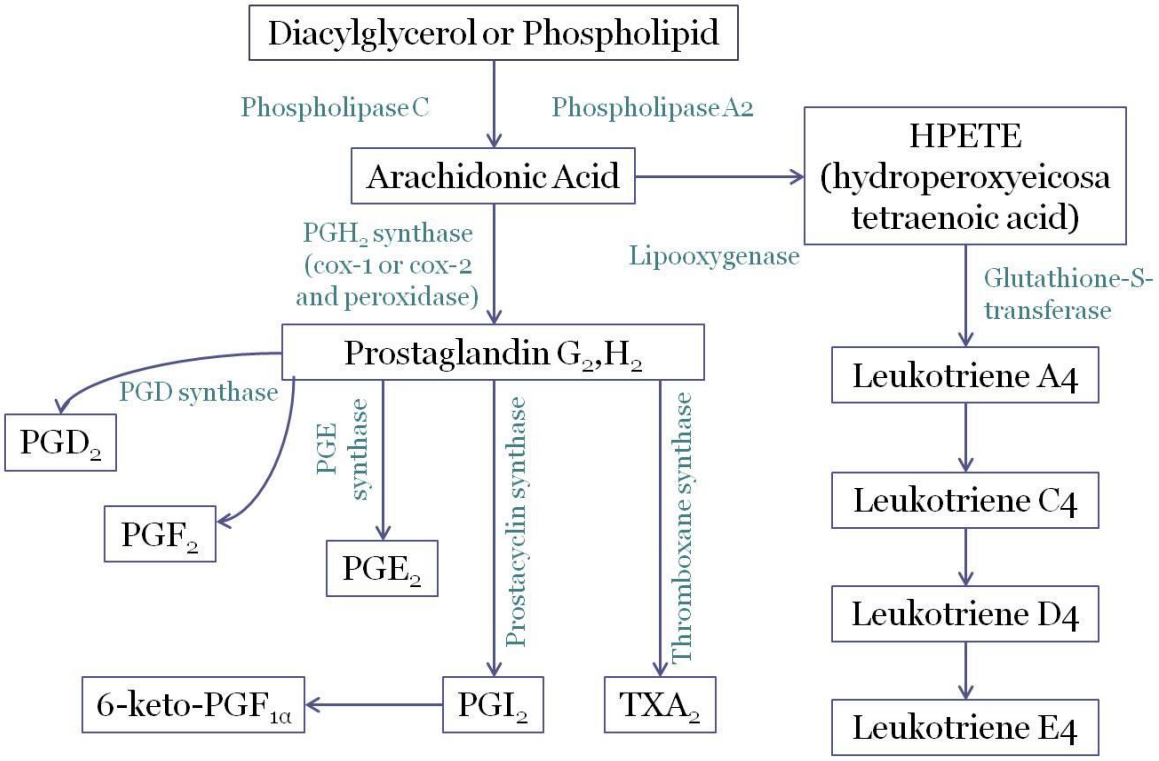
Diacylglycerol or Phospholipid
Phospholipase C
Phospholipase A2
Arachidonic Acid
HPETE (hydroperoxyeicosa tetraenoic acid)
Lipooxygenase
Glutathione-S-transferase
PGH2 synthase (cox-1 or cox-2 and peroxidase)
Prostaglandin G2,H2
PGD synthase
PGE synthase
Prostacyclin synthase
Thromboxane synthase
PGD2
PGF2
PGE2
6-keto-PGF1α
PGI2
TXA2
Leukotriene A4
Leukotriene C4
Leukotriene D4
Leukotriene E4

Figure 3. Prostaglandin E_2 Synthetic Pathway

Schematic of PGE_2 synthesis. Activation of phospholipase A_2 (PLA_2) cleaves a membrane phospholipid into arachidonic acid (AA). AA is then oxidized by cyclooxygenase 1/2 (COX 1/2) to form the unstable intermediates PGG_2 and PGH_2. PGH_2 is then isomerized to different prostaglandin molecules by their respective prostaglandin synthases.

Figure 4

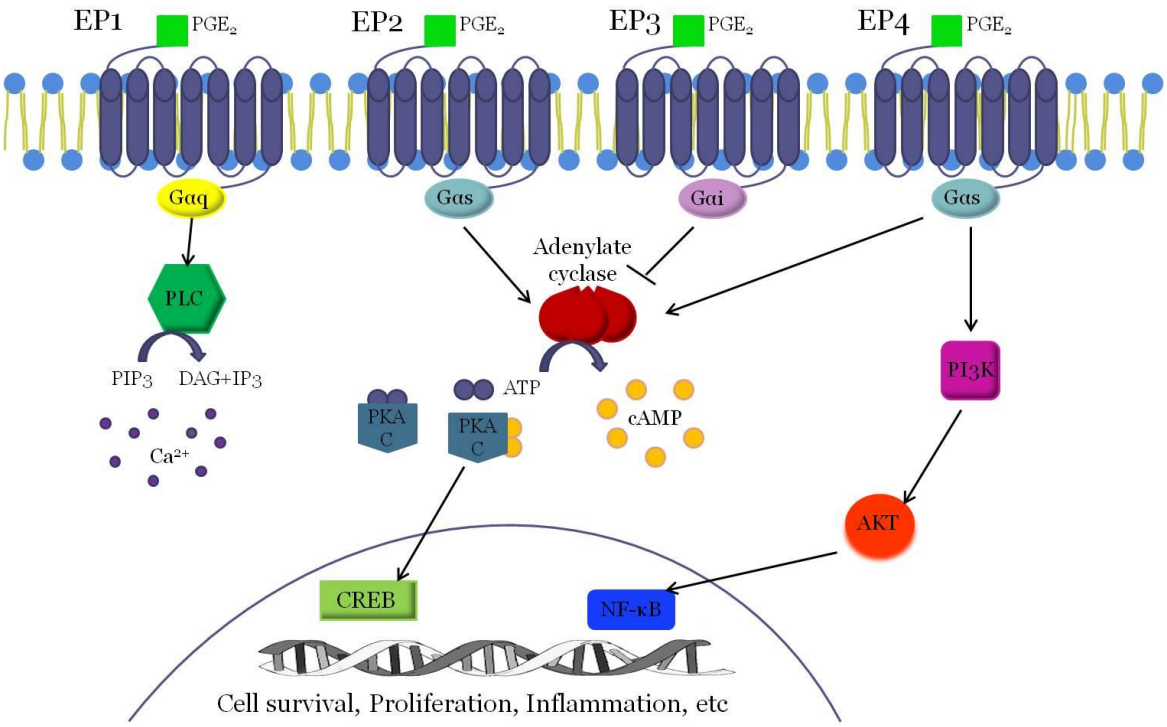
EP1
PGE2
EP2
PGE2
EP3
PGE2
EP4
PGE2
Gαq
Gαs
Gαi
Gαs
Adenylate cyclase
PLC
PIP3
DAG+IP3
Ca2+
ATP
PKA C
PKA C
cAMP
PI3K
AKT
CREB
NF-κB
Cell survival, Proliferation, Inflammation, etc

Figure 4. Prostaglandin E_2 Receptor Signaling

PGE_2 signals through four different EP receptors, EP1-4, which may have similar or opposing effects depending on PGE_2 concentration and EP receptor expression and availability.

PGE_2: Effects on Hematopoiesis and the Niche

Since the 1970s, the role of PGE_2 on hematopoiesis has been extensively investigated. *In vitro* studies by the Pelus laboratory and others showed that PGE_2 acts as a dose-dependent inhibitor of human and murine CFU-GM growth (Pelus *et al.*, 1979; Agiletta *et al.*, 1980; Pelus *et al.*, 1980; Taetle *et al.*, 1980; Taetle and Koessler, 1980; Pelus *et al.*, 1981), and it was determined that PGE_2 plays an important role as a negative regulator of myeloid expansion to counterbalance positive signaling from colony-stimulating factors and thus maintain hematopoietic homeostasis or restore homeostasis following the need for expanded hematopoiesis, i.e. following bacterial infection (Kurland *et al.*, 1978; Kurland *et al.*, 1979). PGE_2 was shown to be most selective for inhibition of colony-forming unit monocyte/macrophage (CFU-M) and CFU-GM and was produced by macrophages in response to macrophage colony-stimulating factor (M-CSF) and granulocyte-macrophage colony-stimulating factor (GM-CSF), creating a feedback inhibition loop (Pelus *et al.*, 1979). Additional studies demonstrated the ability of PGE_2 to increase BFU-E and CFU-GEMM directly (Lu *et al.*, 1984; Nocka *et al.*, 1989) or mediated by factors released from T cells (Lu *et al.*, 1986; Lu *et al.*, 1987; Nocka *et al.*, 1989).

In 1982, the Pelus laboratory demonstrated that short-term exposure of human or murine bone marrow to PGE_2 stimulated the production of cycling CFU-GM from a population of quiescent cells, probably MPP or HSCs. This effect was dependent on time course and concentration of PGE_2 (Pelus, 1982) and was not dependent on cAMP (Pelus, 1984). These and other studies suggest that the kinetics of PGE_2 exposure are crucial for

determining stimulatory versus inhibitory effects on HPC frequency and cell cycle. Within the past few years, PGE_2 was determined to play an important role in development of hematopoiesis in the zebrafish, and *in vitro* pulse exposure to $dmPGE_2$ was shown to increase repopulating capacity of murine bone marrow cells and to increase zebrafish kidney marrow recovery (North *et al.*, 2007), validating the findings of Pelus in 1982 and expanding them to document enhancement of HSC function. In 2009, studies by Hoggatt *et al.* determined that HSPC express all four EP receptors and that short-term, *ex vivo* exposure of HSCs to PGE_2 increased their homing, survival, and proliferation via upregulation of CXCR4, increased entry and progression through cell cycle, and increased production of the anti-apoptotic protein Survivin. Inhibition of PGE_2 signaling via administration of a non-steroidal anti-inflammatory drug (NSAID) results in HSPC egress from the bone marrow. Lack of signaling through the EP4 receptor was shown to drive HPC expansion, causing a greater number of cells to be available for mobilization (Hoggatt *et al.*, 2013b). Alternatively, NSAID-mediated reduction in OPN was implicated in HSC egress from the bone marrow, suggesting that PGE_2 signaling differentially regulates HPC and HSC retention (Hoggatt *et al.*, 2013a). Overall, previous work has elegantly shown that PGE_2 plays an important role in HSPC regulation including retention, migration, survival, proliferation, and engraftment.

In addition to HSPC intrinsic effects, PGE_2 can also have important effects on cells of the hematopoietic niche. In the endosteal niche, PGE_2 is produced by inflammatory M1 macrophages in response to inflammation, infection, or injury and acts to stimulate OB differentiation and bone mineralization (Guihard *et al.*, 2012). *In vitro* studies

suggest that PGE_2 signaling through the EP4 receptor accelerates bone morphogenetic protein (BMP)-induced OB differentiation (Nakagawa *et al.*, 2007). PGE_2 can also affect endothelial cells within the vascular niche by acting directly on the endothelial cell to promote survival, migration, and angiogenesis. *In vitro* studies suggest that PGE_2 binding the EP4 receptor and signaling via extracellular signal-regulated kinase (ERK) phosphorylation induces endothelial cell migration (Rao *et al.*, 2007). Additionally, PGE_2 may signal through the EP4 receptor and the PKA Cγ pathway to promote angiogenesis *in vitro* and *in vivo* (Zhang and Daaka, 2011). PGE_2 directly induces endothelial cell survival and migration by binding the EP2 receptor (Kamiyama *et al.*, 2006) and likely increases signaling through the mammalian target of rapamycin 2 (mTORC2) (Dada *et al.*, 2008).

Chapter 2. Treatment with PGE_2 Facilitates Hematopoietic Recovery Post-Irradiation

Introduction:

The highly proliferative nature of the hematopoietic system required to maintain homeostasis makes HSPC highly sensitive to radiation damage (Till and McCulloch, 1964; Broxmeyer *et al.*, 1976; Chinsoo and Glatstein, 1998; Chitetti *et al*., 2011). Total body irradiation and chemotherapy, as well as the risk of radiation accident, create a need for increased countermeasures to promote hematopoietic recovery after exposure to radiation or chemotherapeutic drugs. The hematopoietic system does recover after chemotherapy and radiotherapy, but heavily treated patients show reduced tolerance to additional therapy and lower baseline levels of circulating blood cells and clotting factors, particularly platelets. (Mauch *et al.*, 1995). Decreased marrow function that persists for up to 5 years flowing irradiation has been reflected by marrow densitometry scanning (Rubin *et al.*, 1973) as well as by enumeration of CFU-GM (Lohrmann and Schreml, 1988).

Substantive damage to the bone marrow from radiation exposure results in the hematopoietic syndrome of the acute radiation syndrome (HS-ARS), which is characterized by life-threatening neutropenia, lymphocytopenia, thrombocytopenia, and possible death due to infection and/or hemorrhage. HSPC are sensitive to radiation exposure, but surviving populations of these cells can restore hematopoiesis if given time to repair DNA damage, self-renew, expand, and differentiate. In the case of accidental radiation exposure, the dose of radiation exposure for individuals may be

unknown and differences in patient age and health status complicate the efficiency of treatment. Patients who are exposed to radiation doses between 2-6 Gy are most amendable to treatment, but in the absence of treatment nearly all those exposed to 4 Gy or higher will die within 30 days. Casualties exposed to doses that exceed 6-8 Gy will likely have thermal or blast injuries that preclude survival (Anno *et al.*, 1989). In the context of a radiation accident, an effective radiomitigative agent should be easily administered, stable, able to be rapidly distributed, allow a window of efficacy, and be able to mitigate or reduce the severity of HS-ARS in patients exposed to high doses of irradiation, while remaining benign to those who received limited to no exposure.

Life-threatening effects of mid-high level radiation exposure result from DNA damage that triggers processes leading to cell cycle arrest and apoptosis, loss of genomic stability or epigenetic processes in descendant cells, and from indirect toxic effects mediated by abnormal signaling and function of the bone marrow microenvironment (Till and McCulloch, 1964; Broxmeyer *et al.*, 1976; Coleman *et al.*, 2003; Daniak *et al.*, 2003; MacVittie *et al.*, 2005). As discussed previously, the eicosanoid molecule PGE_2 has positive effects on HSCs by decreasing apoptosis through upregulation of Survivin and increasing self-renewal, while dose-dependently inhibiting proliferation and expansion of HPCs. Based on the known pleiotropic effects of PGE_2 signaling, we investigated the ability of the metabolically stable analog of PGE_2, $dmPGE_2$, to act as a radiomitigator and promote recovery of the HSPC populations after radiation damage.

Materials and Methods:

Mice

C57Bl/6 mice were purchased from the Jackson Laboratory (Bar Harbor, ME) and maintained in the Indiana University School of Medicine (IUSM) Animal Facility. All mouse experiments were approved by the Institutional Animal Care and Use Committee (IACUC).

Irradiation

Mice were placed in single chambers of a plexiglass irradiation pie (Braintree Scientific, Braintree, MA), with up to 10 mice per pie. Each group of mice irradiated within the same pie were evenly distributed among all treatment groups to ensure that each group received the same irradiation exposure conditions. Mice were irradiated with a ^{137}Cesium gamma radiation source (Mark I model 68A; JL Shepherd and Associates, San Fernando, CA) at an exposure rate of 108 cGy per minute for a total of 896 cGy (lethal dose (LD) 70/30) or 650 cGy (sublethal irradiation).

Post-Irradiation Treatment

Irradiated mice were treated with either a single subcutaneous dose (200 µL) of vehicle or dmPGE$_2$ (Cayman Chemical, Ann Arbor, MI) (35 µg per mouse) at 24 hours post-irradiation.

Morbidity and Mortality Monitoring

Mice were observed for morbidity or mortality twice daily after irradiation for a total of 30 days. Moribund mice were scored for signs of suffering based on a three-point, three parameter scale: severity of hunched posture, squinted/closed eyes, and activity level. Moribund mice with a score of 8 or 9 were humanely euthanized and the date of death recorded.

Methylcellulose Colony Assays

Bone marrow cells were collected from long bones, flushed, counted and plated at concentrations of 20,000, 50,000, or 100,000 cells per plate in 1% methylcellulose as described (Broxmeyer *et al.*, 2007; Fukuda *et al.*, 2007) and incubated at 37°C, 5% CO_2 and 5% O_2 for 7 days. Total CFC including CFU-GM, BFU-E, and CFU-GEMM were enumerated.

Flow Cytometry Analysis

Bone marrow cells were harvested from the long bones of mice and a single-cell suspension prepared in PBS with 2% HI-FBS (Thermo Scientific HyClone, Logan, UT). Total nucleated cell counts were obtained using a Hemavet-950 (Drew Scientific, Dallas, TX). Antibodies were purchased from BD Biosciences unless otherwise noted (San Jose, CA). For detection of mouse LSK cell populations, Lineage-VD450, Sca-1-PE, and c-kit-APC antibodies were used. For SLAM-LSK cell detection the staining profile CD150-PE-Cy5, CD48-Fitc, Lin-VD450, Sca-1-PE, and c-kit-APC was used. For analysis of Survivin

levels in LSK and SLAM-LSK cells the following staining profile was used: Survivin-PE, Lin-VD450, Sca-1-APC, c-kit-APC-cy7, CD150-PE-Cy5, and CD48-FITC. Events were collected using an LSRII flow cytometer (BD Biosciences) and analysis was performed using CellQuest (BD Biosciences) or FlowJo (Tree Star, Inc. Ashland, OR).

Data Analysis

Data were analyzed by Student's T-test using Microsoft Excel unless otherwise noted.

Results:

dmPGE$_2$ Treatment Increases Survival Post-Irradiation

Endogenous PGE$_2$ synthesis is upregulated following irradiation (Chen *et al.*, 1996) with PGE$_2$ levels rising in the bone marrow by day 8 post-irradiation, as a result of increased levels of COX 1/2 (Hoggatt *et al.*, 2013b). Since PGE$_2$ is produced endogenously in response to irradiation, we hypothesized that this could represent a possible protective mechanism, due to the known abilities of PGE$_2$ to promote HSC survival and proliferation. We also reasoned that addition of exogenous PGE$_2$ may further contribute to restoration of HSC function. Therefore, we assessed the ability of exogenous administration of the metabolically stable PGE$_2$ analog dmPGE$_2$ to mitigate the effects of irradiation and accelerate restoration of hematopoiesis.

In order to assess the ability of dmPGE$_2$ to mitigate radiation damage to the bone marrow, we used a murine model of the hematopoietic syndrome of acute

radiation syndrome (HS-ARS) developed by Dr. Orschell at IUSM (Chua *et al.*, 2012; Plett *et al*., 2012). Mice (n=20 per group) were irradiated at 865 cGy and treated with vehicle or $dmPGE_2$ (35 µg per mouse) at 24 hours post-irradiation and morbidity/mortality monitored for 30 days following irradiation. Single treatment with $dmPGE_2$ at 24 hours post-irradiation resulted in 70% survival ($p<0.05$) compared to only 30% survival of vehicle control mice (Figure 5A). Analysis of HPC potential by clonogenic assay at 30 days post-irradiation demonstrated a significant deficit in CFC in both vehicle and $dmPGE_2$-treated mice compared to non-irradiated controls, while distribution among CFU-GM, BFU-E, and CFU-GEMM colony formation remained equivalent across all groups. However, CFC in $dmPGE_2$-treated mice showed greater recovery than in vehicle mice (Figure 5B). Analysis of bone marrow cellularity by flow cytometry at 30 days post-irradiation revealed significantly increased numbers of LSK HPC in $dmPGE_2$-treated mice ($p=0.03$) compared to vehicle control. SLAM-LSK numbers although trending higher in the $dmPGE_2$-treated group were not significantly different than vehicle. Together these studies suggest that $dmPGE_2$ has the potential to be an effective radiomitigative agent that promotes hematopoietic recovery.

Figure 5

A

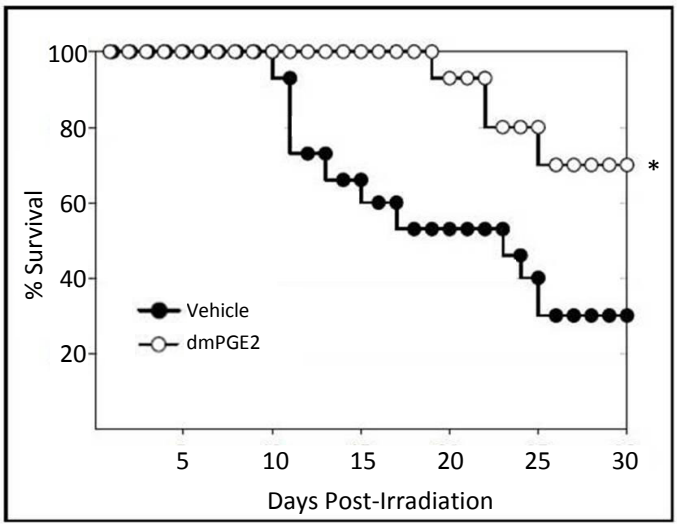
100
80
60
40
20
% Survival
Vehicle
dmPGE2
*
5
10
15
20
25
30
Days Post-Irradiation

B

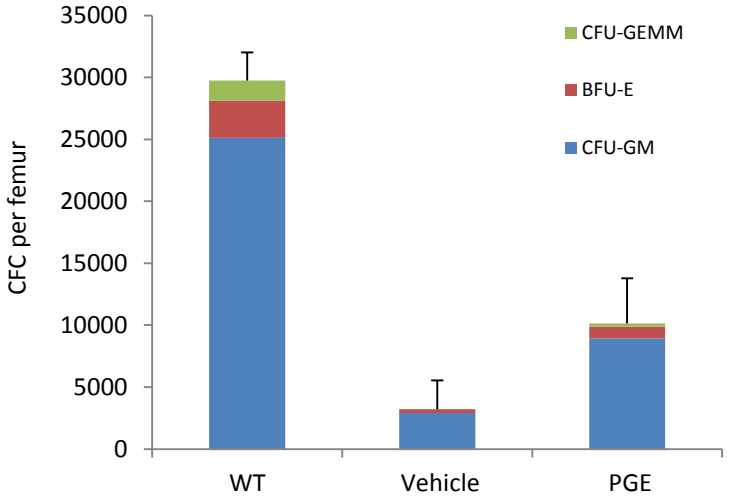
35000
30000
25000
20000
15000
10000
5000
0
CFC per femur
CFU-GEMM
BFU-E
CFU-GM
WT
Vehicle
PGE

C

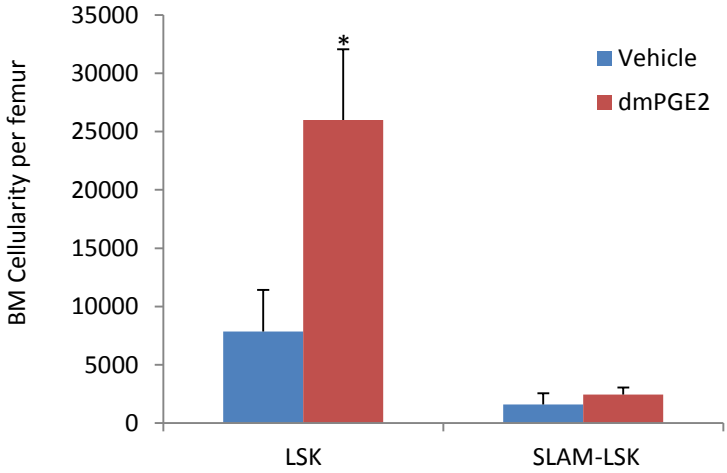
35000
30000
25000
20000
15000
10000
5000
0
BM Cellularity per femur
*
Vehicle
dmPGE2
LSK
SLAM-LSK

Figure 5. Radiomitigation by Treatment with $dmPGE_2$

A) Cohorts of 20 mice were irradiated with 865 cGy from a ^{137}Cs source. Mice received a single dose of $dmPGE_2$ (35 μg) or vehicle 24 hours after irradiation. Animals were monitored for morbidity and mortality twice daily for 30 days. Survival curves were analyzed with a log-rank test; * = $p < 0.05$.

B) Analysis of total CFU-GM, BFU-E, and CFU-GEMM in methylcellulose culture at 30 days post-irradiation. Data are mean ± SEM, n=4 mice per group, each assayed individually.

C) Analysis of bone marrow cellularity by flow cytometry at 30 days post-irradiation. Data are mean ± SEM, n=3 mice per group, analyzed by Student's t-test; * = $p < 0.05$.

dmPGE$_2$ Promotes Hematopoietic Recovery in a Sub-Lethal Model of Irradiation

Since treatment with dmPGE$_2$ promotes survival and recovery after LD 70/30 irradiation, we investigated hematopoietic recovery after sublethal damage to the bone marrow. Mice were irradiated at 650cGy, treated with dmPGE$_2$ or vehicle control at 24 hours post-irradiation, and HSPC populations analyzed at day 2, 7, 10, and 14 post-irradiation using clonogenic assay and flow cytometric analysis. Analysis of clonogenic HPC potential demonstrated that HPC recovery in dmPGE$_2$-treated mice occurs significantly faster than vehicle control by 10 days post-sublethal irradiation ($p<0.05$), increasing to an even greater extent by 14 days post-irradiation ($p<0.05$) (Figure 6A). Despite faster recovery, CFC in all irradiated mice were still considerably lower than in non-irradiated control mice.

Analysis of HSPC populations by flow cytometry revealed that at day 2 post-irradiation, LSK cell number is significantly lower in mice treated with dm-PGE$_2$ than vehicle control ($p<0.05$). However, greater recovery of the LSK population is seen in the dmPGE$_2$-treated group by 14 days post-irradiation ($p<0.05$) (Figure 6B). SLAM-LSK cell numbers remained similar across treatment groups until day 14 when dm-PGE$_2$-treated mice demonstrate greater recovery of the SLAM-LSK cell population ($p<0.05$) (Figure 6C).

Figure 6

A

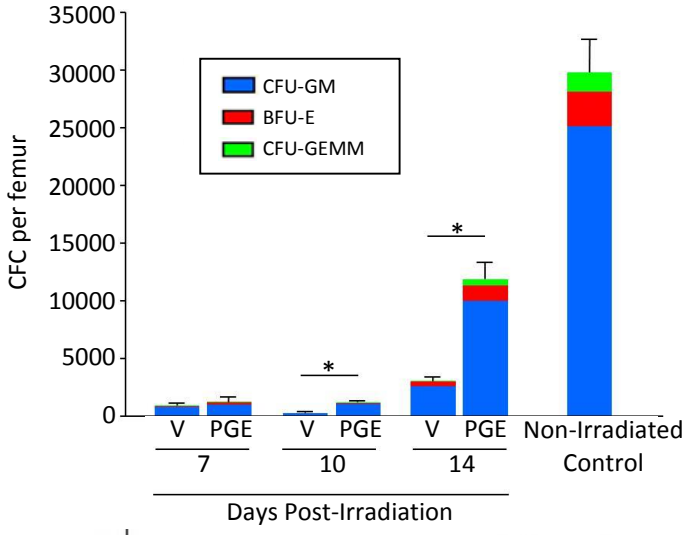
35000
30000
25000
20000
15000
10000
5000
0
CFC per femur
CFU-GM
BFU-E
CFU-GEMM
*
*
*
V PGE V PGE V PGE Non-Irradiated
7 10 14 Control
Days Post-Irradiation

B

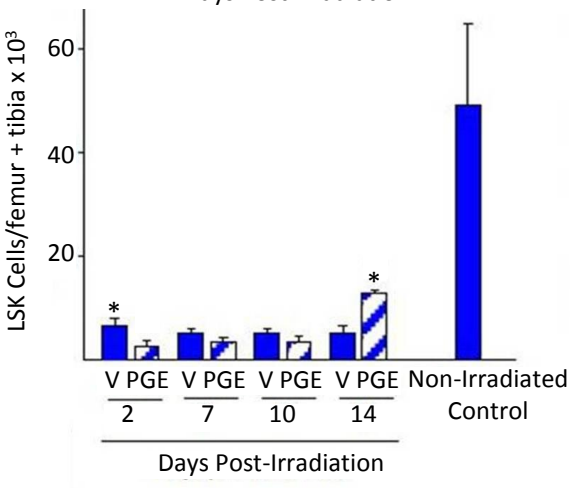
60
40
20
LSK Cells/femur + tibia x 10³
*
*
V PGE V PGE V PGE V PGE Non-Irradiated
2 7 10 14 Control
Days Post-Irradiation

C

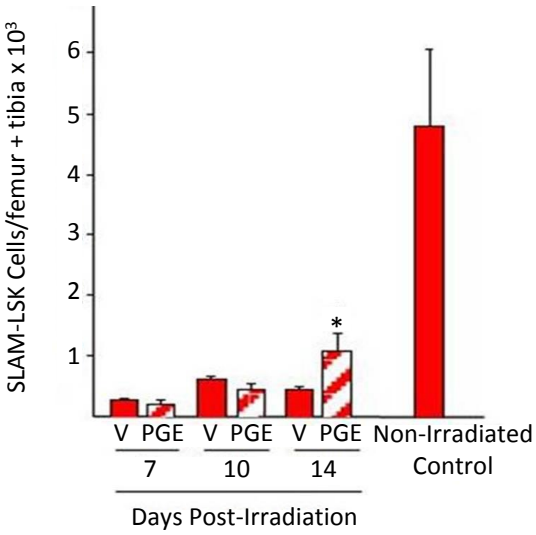
6
5
4
3
2
1
SLAM-LSK Cells/femur + tibia x 10³
*
V PGE V PGE V PGE Non-Irradiated
7 10 14 Control
Days Post-Irradiation

Figure 6. dmPGE$_2$ Facilitates HSPC Recovery Post-Irradiation

A) Cohorts of mice (n=12 per group) were irradiated at 650 cGy, treated with dmPGE$_2$ or vehicle 24 hours post-irradiation, and bone marrow cell HPC populations analyzed for CFU-GM, BFU-E, and CFU-GEMM in methylcellulose at day 7, 10, and 14 (n=3 per day, per group) post-irradiation. Hematopoietic recovery was also compared to non-irradiated control mice. Data are mean ± SEM, analyzed by Student's t-test; * = $p < 0.05$.

B) Analysis of LSK cell number by flow cytometry. Data are mean ± SEM, n=3 mice per group, analyzed by Student's t-test; * = $p < 0.05$.

C) Analysis of SLAM-LSK cell number by flow cytometry. Data are mean ± SEM, n=3 mice per group, analyzed by Student's t-test; * = $p < 0.05$.

Together these studies suggest that treatment with dmPGE_2 post-irradiation facilitates hematopoietic recovery, but it has not yet been determined if the mechanism of action is HSPC intrinsic or mediated through extrinsic repair of the bone marrow microenvironment. PGE_2 is known to increase HSPC survival through upregulation of the anti-apoptotic factor Survivin, as discussed previously. In order to investigate if PGE_2 promotes hematopoietic recovery after radiation damage via increased Survivin expression, mice were irradiated at 650 cGy, treated with vehicle or dmPGE_2 at 24 hours post-irradiation, and femurs harvested at three different time-points after irradiation: 36 hours, 48 hours, and 60 hours. Cells collected were analyzed via flow cytometry for LSK and SLAM-LSK cell number and Survivin levels within the LSK and SLAM-LSK populations. LSK (Figure 7A) and SLAM-LSK (Figure 7B) cell number were higher in vehicle-treated mice ($p<0.05$) compared to mice treated with dmPGE_2. At all measured time points, Survivin levels were similar between vehicle and dmPGE_2-treated mice in both LSK and SLAM-LSK cell populations (Figure 7C).

Figure 7

A

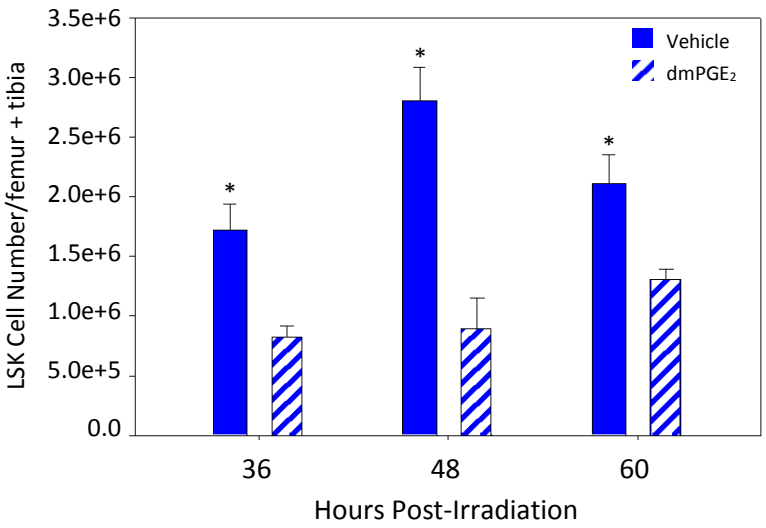
3.5e+6
3.0e+6
2.5e+6
2.0e+6
1.5e+6
1.0e+6
5.0e+5
0.0
LSK Cell Number/femur + tibia
Vehicle
dmPGE2
*
*
*
36
48
60
Hours Post-Irradiation

B

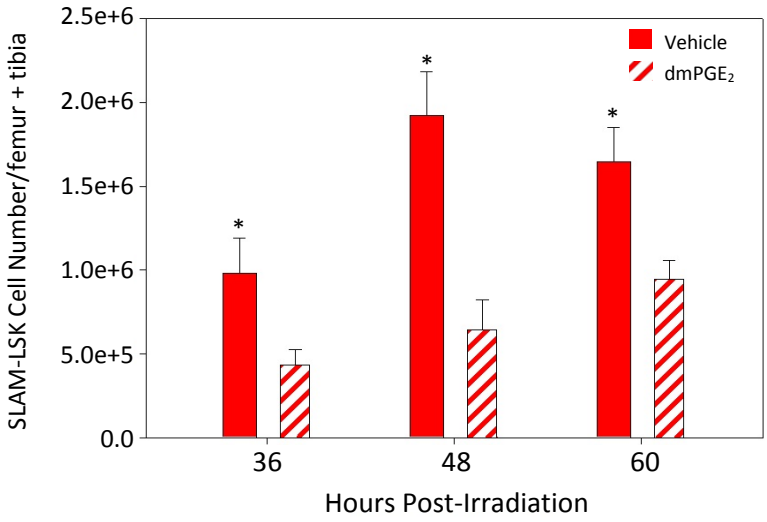
2.5e+6
2.0e+6
1.5e+6
1.0e+6
5.0e+5
0.0
SLAM-LSK Cell Number/femur + tibia
Vehicle
dmPGE2
*
*
*
36
48
60
Hours Post-Irradiation

C

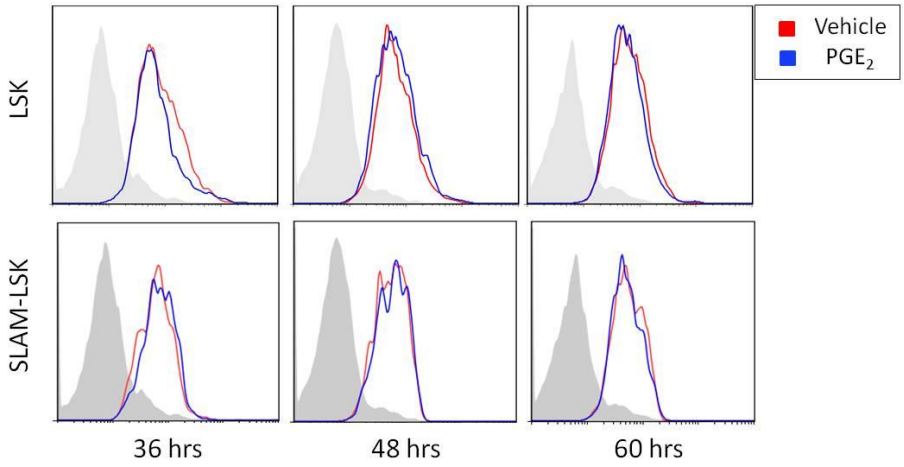
LSK
SLAM-LSK
Vehicle
PGE2
36 hrs
48 hrs
60 hrs

Figure 7. dmPGE$_2$ Treatment Post-Irradiation does not Increase Survivin Levels in HSPC

A) Mice (n=9 per group) were irradiated at 650 cGy and treated with vehicle or dmPGE$_2$ at 24 hours post-irradiation. LSK cell number was analyzed by flow cytometry at 36, 48, and 60 hours post-irradiation. Data are mean ± SEM, n=3 mice per group, analyzed by Student's t-test; * = $p < 0.05$.

B) Analysis of SLAM-LSK cell number by flow cytometry at 36, 48, and 60 hours post-irradiation. Data are mean ± SEM, n=3 mice per group, analyzed by Student's t-test; * = $p < 0.05$.

C) Analysis of Survivin levels within LSK and SLAM-LSK cell populations of vehicle and dmPGE$_2$-treated mice at 36, 48, and 60 hours post-irradiation; * = $p < 0.05$.

Discussion:

These studies outline the ability of PGE_2 to act as a radiomitigating agent, both in the context of LD 70/30 irradiation and sublethal irradiation. Numerous studies have shown that PGE_2 and prostaglandin analogs may act as radioprotectants that prevent DNA damage and promote survival of non-cycling cells (Zaffaroni *et al.*, 1993; van Buul *et al.*, 1999) in a variety of cell types and tissues, including the hair follicle (Malkinson *et al.*, 1993) and the intestine (Hanson and Collins, 1992), but their ability to mitigate the effects of radiation damage remains underexplored.

Studies performed by our laboratory and others have investigated the potential radiomitigative effect of NSAID treatment. Hofer *et al.* (2006) demonstrated increased hematopoietic recovery in mice after sublethal irradiation and subsequent administration of Meloxicam beginning at 24 hours post-irradiation and continuing treatment once daily for 4 days after irradiation. A similar study by our laboratory confirmed these results in lethally irradiated mice, showing increased survival and enhanced hematopoietic recovery with NSAID administration 48 hours after irradiation, with treatment continuing for a total of 4 days (Hoggatt *et al.*, 2013b). Conversely, additional studies have demonstrated that NSAID administration immediately following irradiation is detrimental, resulting in decreased survival (Jiao *et al.*, 2009).

Together, our results combined with previous studies highlight an important role for PGE_2 signaling in hematopoietic recovery from radiation injury. PGE_2 is known to be produced endogenously in response to irradiation (Chen *et al.*, 1996; Hoggatt *et al.*, 2013b) and supplementation with exogenous $dmPGE_2$ at 6 hours (Hoggatt *et al.*, 2013b)

or 24 hours after irradiation, promotes recovery of the hematopoietic system, suggesting that PGE_2 is vital to hematopoiesis at early time points post-irradiation. Alternatively, blockage of PGE_2 signaling through NSAID administration at early time points after irradiation decreases survival and recovery of hematopoiesis (Hoggatt *et al.*, 2012), but delaying NSAID administration to 24-48 hours after irradiation and continuing treatment for several days promotes survival and hematopoietic recovery.

Based on these results, and consistent with the published literature regarding the need to consider duration of PGE exposure, we have formed a "just right" hypothesis for PGE_2 signaling and post-irradiation recovery and survival. Too little PGE_2 at early time periods post-irradiation reduces positive anti-apoptotic and self-renewal effects, while too much PGE_2 at later time points likely inhibits HPC expansion and reduces hematopoietic recovery. Early exposure to PGE_2 may be important for HSPC survival by promoting survival and DNA repair mechanisms, while initially inhibiting HPC expansion to allow for DNA repair. Our results indicate that within the first 36-60 hours after irradiation, treatment with $dmPGE_2$ may not cause an increase in production of the anti-apoptotic factor Survivin within the HSPC populations. However, PGE_2 signaling may also facilitate hematopoiesis by promoting recovery of the HSC niche. Therefore, further studies were designed to investigate the role of PGE_2 in niche repair.

Chapter 3: PGE_2 Promotes Repair of the HSC Niche after Irradiation

Introduction:

We have demonstrated the ability of $dmPGE_2$ to act as a radiomitigative agent, promoting survival and facilitating recovery of HSPC populations. It is yet unknown whether the radiomitigative effect of PGE_2 is HSPC intrinsic, extrinsic (mediated through the bone marrow microenvironment), or both. As discussed, PGE_2 plays an important role in several components of the HSC niche, including stimulation of OB differentiation (Nakagawa *et al.*, 2007) and bone mineralization (Guihard *et al.*, 2012) and enhancement of endothelial cell migration and survival (Kamiyama *et al.*, 2006; Rao *et al.*, 2007; Dada *et al.*, 2008; Zhang and Daaka., 2011). This suggests that PGE_2 may mitigate the effects of radiation damage by promoting recovery or survival of niche components such as OBs and sinusoidal endothelial cells.

Additional studies have shown that at 48 hours post-irradiation surviving megakaryocytes are observed closer to the endosteal surface of bone rather than distributed throughout the bone marrow (Dominici *et al.*, 2009). This megakaryocyte localization with the endosteum is accompanied by increased levels of SDF-1 and megakaryocyte-derived factors PDGF-β and bFGF. Since we previously reported that PGE_2 can upregulate expression of the receptor for SDF-1, CXCR4, at least in HSPC (Hoggatt *et al*., 2009), and that PGE_2 is produced endogenously in response to irradiation (Chen *et al.*, 1996; Hoggatt *et al.*, 2013b), and since it has been reported that MKs can stimulate OB proliferation (Kacena *et al*., 2006), we hypothesized that

supplementation with exogenous $dmPGE_2$ may increase expression of MK CXCR4 and, subsequently, increase MK migration or enhance MK survival, and further augment the effect of the MK on niche restoration. To investigate the effects of PGE_2 on MK migration, we analyzed the effect of irradiation, irradiation with $dmPGE_2$ treatment, and irradiation with NSAID administration (abrogation of PGE_2 signaling) on the bone marrow microenvironment, as well as the effect of $dmPGE_2$ on CXCR4 levels and MK migration *in vitro*.

Materials and Methods:

Mice

C57Bl/6 mice were purchased from the Jackson Laboratory (Bar Harbor, ME) and maintained in the Indiana University School of Medicine (IUSM) Animal Facility. All mouse experiments were approved by the Institutional Animal Care and Use Committee (IACUC).

Irradiation

Mice were placed in single chambers of a plexiglass irradiation pie (Braintree), with up to 10 mice per pie. Each group of mice irradiated within the same pie was evenly distributed among all treatment groups to ensure that each group received the same irradiation exposure conditions. Mice were irradiated with a ^{137}Cesium gamma radiation source for a total of 650 cGy (sublethal irradiation).

Post-Irradiation Treatment

Groups of 10 irradiated mice were treated with either a single subcutaneous dose of vehicle, dmPGE_2 (35 µg per mouse) at 24 hours post-irradiation, or 6mg/kg Meloxicam dosed immediately after irradiation and again 24 hours after irradiation.

Histological Analysis

Femurs were collected and immediately fixed in a solution of 4% paraformaldehyde at 4°C for 24 hours and stored in 70% ethanol at 4°C until decalcification. Bones were decalcified in a stirred solution of 10% ethylenediaminetetraacetic acid (EDTA) at 4°C and pH 7.4 for a period of two weeks. After decalcification bones were embedded in paraffin, sectioned, and stained using hematoxylin and eosin. Sections were visualized with a Leica DM2500 microscope outfitted with micropublisher Q-imaging camera (W. Nuhsbaum Inc., McHenry, IL). Forty-eight 1x1 images were captured at 200x and stitched into a composite image (Figure 8A). MK distance from the endosteum of cortical bone (Figure 8B) was calculated using a BioQuant Osteo software automated measuring system (Bioquant Imaging Corporation, Nashville, TN) and normalized to mm of bone surface.

Megakaryocyte Expansion

Bone marrow cells from the long bones of two mice were flushed from femurs using DMEM with 2% HI-FBS. Whole bone marrow cells were then enriched for the Lin^- population using a lineage depletion kit. Lin^- cells were then cultured in DMEM with 10%

HI-FBS, 10% penicillin+streptomycin, and 100 ng/mL TPO and incubated at 37°C, 5% CO_2 and 5% O_2 for 7 days to expand megakaryocytes.

Flow Cytometry Analysis

Bone marrow cells were harvested from the long bones of mice and a single-cell suspension established in PBS with 2% HI-FBS (Thermo Scientific HyClone, Logan, UT). Total nucleated cell counts were obtained using a Hemavet-950 (Drew Scientific, Dallas, TX). Antibodies were purchased from BD Biosciences unless otherwise noted. For detection of mouse MK populations, cells were lineage depleted and stained with Lin-VD450, CD41-Fitc, and CXCR4-PE. Events were collected using an LSRII flow cytometer (BD Biosciences) and analysis was performed using CellQuest (BD Biosciences) or FlowJo (Tree Star, Inc. Ashland, OR).

Migration Assays

Chemotaxis of Lin^- $CD41^+$ MKs was determined using a two-chamber Costar Transwell (6.5mm diameter, 8μm pore; Cambridge, MA) system. Cells from MK expansion cultures were treated with vehicle or $dmPGE_2$ (1μM) for 2 hours at 37°C with 5% CO_2, washed twice, and then cultured in RPMI+10% HI-FBS overnight to allow for upregulation of CXCR4. Following incubation, cells were washed and resuspended at $1x10^6$ cells/mL in RPMI+0.5% BSA. One hundred thousand cells were added to the top chamber of the transwell with 100 ng/mL rmSDF-1 (R&D Systems, Minneapolis, MN) in the bottom chamber. Cells were incubated for 4 hours at 37°C in order for migration to occur. Total

migrated cells in the bottom chamber were collected, stained for lineage markers and CD41, and cell events were obtained for 30 seconds via flow cytometer. Total percent migration was calculated by dividing the total live cell counts in the lower well by the cell input multiplied by 100. Cells were stained for Lin and CD41 to determine percent migration of Lin^- $CD41^+$ cells.

Data Analysis

Data were analyzed by Student's T-test using Microsoft Excel unless otherwise noted.

Figure 8

A

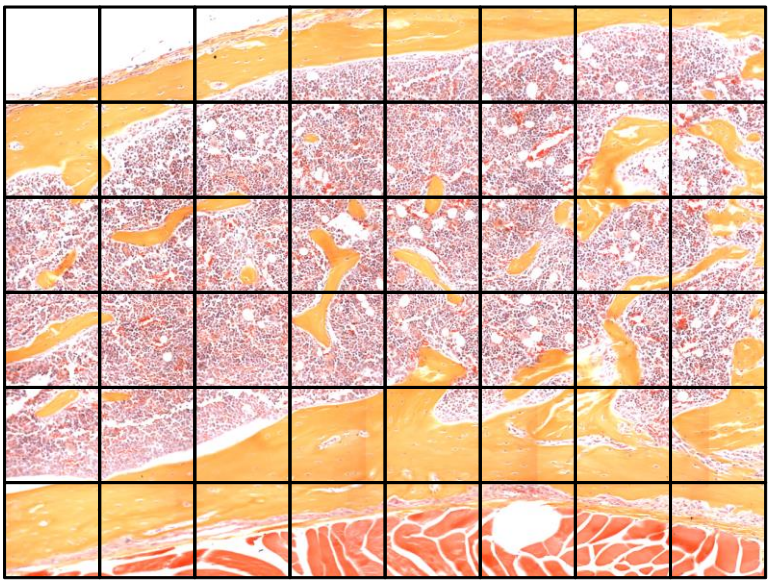

B

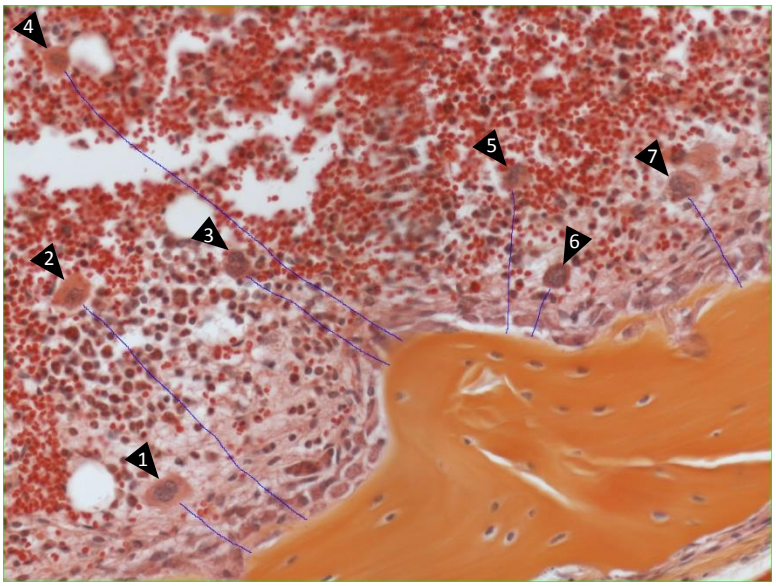

MK	Distance (µm)
1	34.07
2	123.66
3	52.04
4	167.39
5	45.53
6	19.36
7	38.81

Figure 8. Schematic of Histological Analysis

A) Forty-eight 1x1 images were captured at 200x magnification using a Q-imaging camera attached to a Leica microscope. These images were stitched together using BioQuant Osteo software to form a composite image of each femur section.

B) Representative image showing how MK number and distance to the endosteum of cortical bone were analyzed. Total MK number per mm of bone and MK distance to the endosteum were quantified using BioQuant Osteo software. The distance from each MK to the nearest cortical bone surface was measured within a defined area of the femur shaft allowing MK number to be normalized to mm of bone surface.

Results:

PGE_2 Increases MK Association with the Endosteum Post-Irradiation

In order to investigate the effect of irradiation and post-irradiation treatment on the bone marrow niche, femurs were collected from non-irradiated control mice (n=8) and from sublethally irradiated mice treated at 24 hours post-irradiation with either vehicle (n=7), $dmPGE_2$ (n=9), or NSAID (n=9). At 48 hours post-irradiation, 24 hours after drug treatment, histological analysis demonstrated marked changes in bone marrow cellularity between non-irradiated control mice (Figure 9A) and vehicle treated mice (Figure 9B). Loss of white blood cells and increase in erythrocytes (blue arrow) were observed within the irradiated mouse bone marrow. An increase in OB cell number can also be seen in the irradiated mouse (blue box) with OBs creating a layer two-three cells high along the endosteal surface of cortical bone. In a non-irradiated control mouse, OBs form a single layer along the endosteum (Figure 10A,B) and MKs (black arrows) are distributed evenly throughout the bone marrow, with very few found in close proximity to the endosteum (Figure 10A,B). This increase in OBs along the endosteum validates the findings of Dominici *et al.,* 2009.

In irradiated mice, an increase in OB cell number along the endosteum is seen in all groups, regardless of drug treatment (Figures 11, 12, 13; blue boxes). As reported previously reported, there is an increase in MK association with the endosteum following irradiation (Figure 11; black arrows indicate MK). Treatment with $dmPGE_2$ enhanced the number of MK associated with the endosteum of cortical bone (Figures

12; black arrows), whereas blocking endogenous PGE_2 with the NSAID Meloxicam appears to significantly abrogate this effect (Figure 13; black arrows).

Figure 9

A

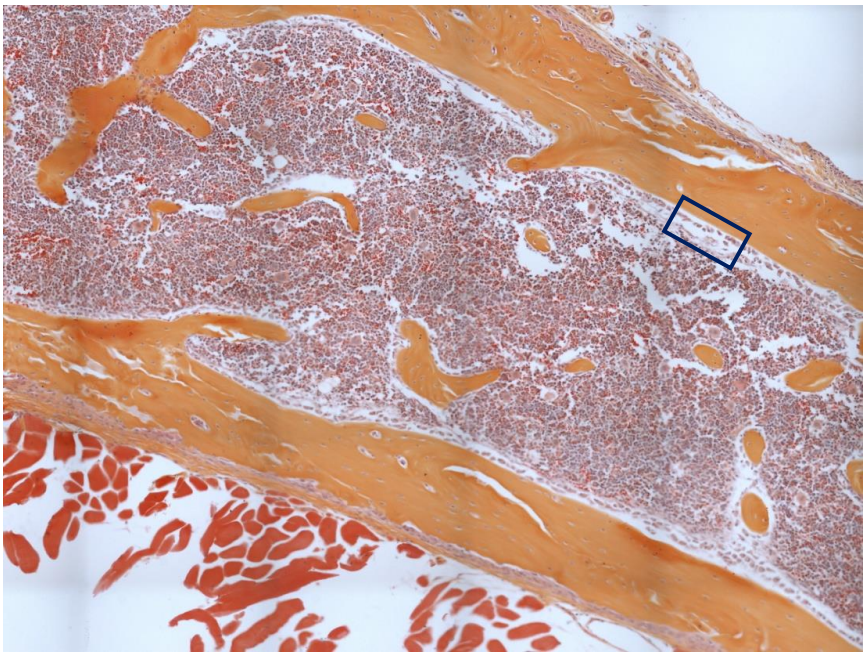

B

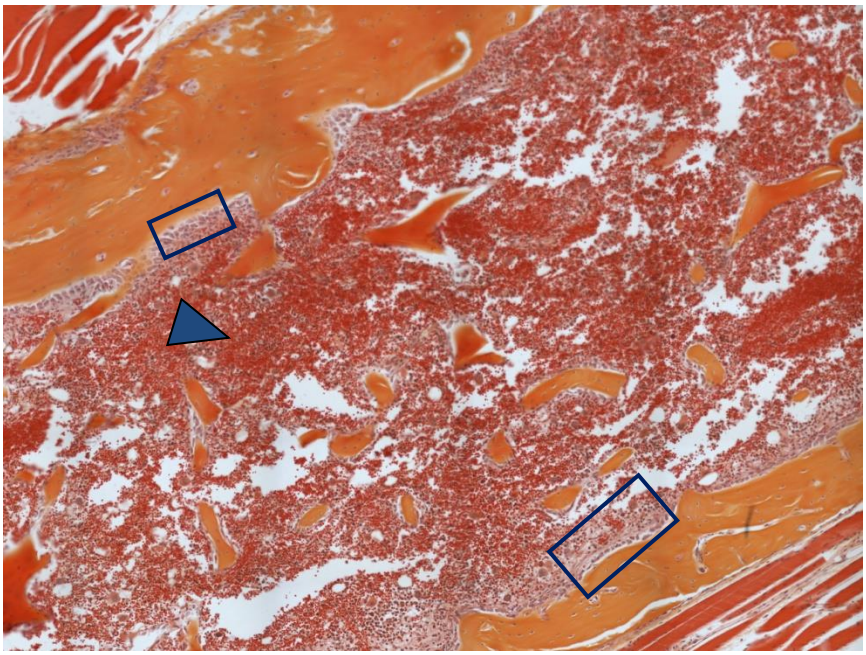

Figure 9. Representative Images from Control and Irradiated Mice

A) Femurs were harvested, fixed, paraffin-embedded, sectioned and stained with hemotoxylin and eosin from non-irradiated control mice (n=8). A representative image shows normal pathology for a mouse femur section.

B) Mice (n=7) were irradiated at 650 cGy, treated with vehicle 24 hours post-irradiation, and femurs harvested at 48 hours post-irradiation. Staining with hemotoxylin and eosin shows marked changes in bone marrow cellularity between this irradiated mouse femur and the non-irradiated control mouse femur. Note the increase in erythrocytes (blue arrow) and striking increase in OB cell number (blue box).

Figure 10

A

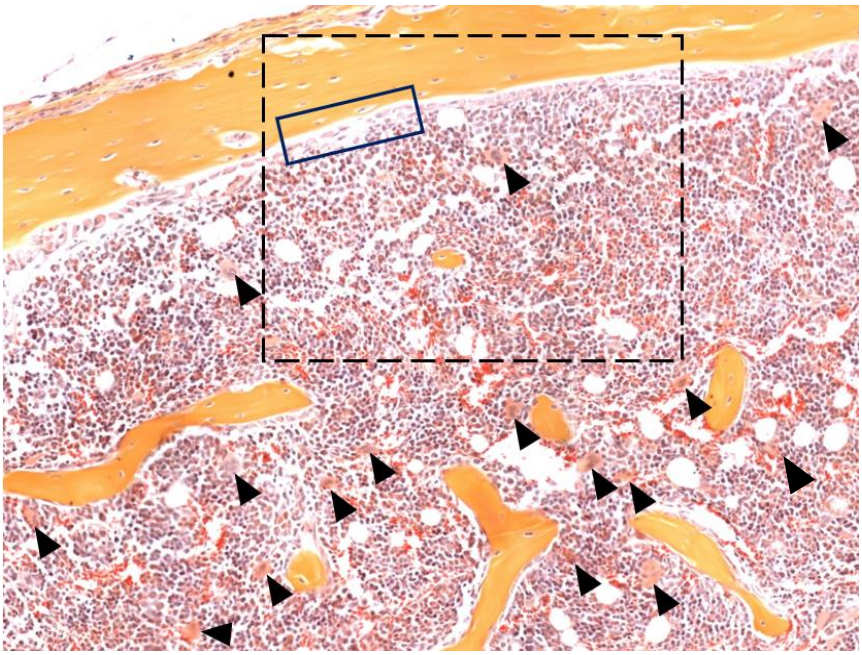

B

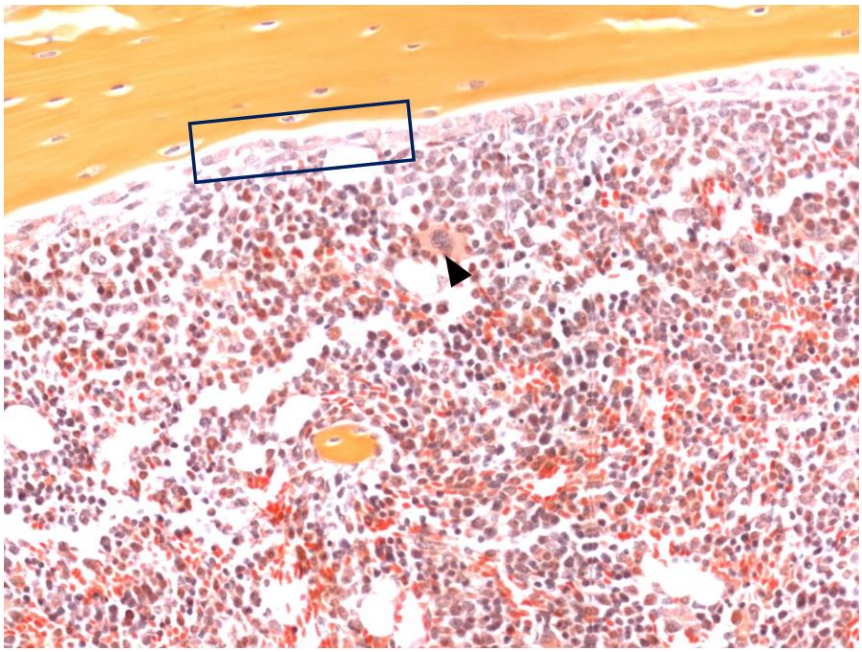

Figure 10. Representative Images from a Non-Irradiated Control Mouse

A) Femurs were harvested from non-irradiated control mice (n=8), fixed, decalcified (two weeks), paraffin-embedded, sectioned, and stained with hemotoxylin and eosin. A representative image shows normal pathology for a mouse femur section. MKs (black arrows) are found within the bone marrow and are not localized or closely associated with the endosteum. OBs are found in a single layer along the endosteum (blue box). The dashed lines indicate which region of this section has been magnified in 10B.

B) A representative femur section from a non-irradiated control mouse shown at 200x magnification. One MK (black arrow) is present in this view. Note the single layer of OBs along the endosteum (blue box).

Figure 11

A

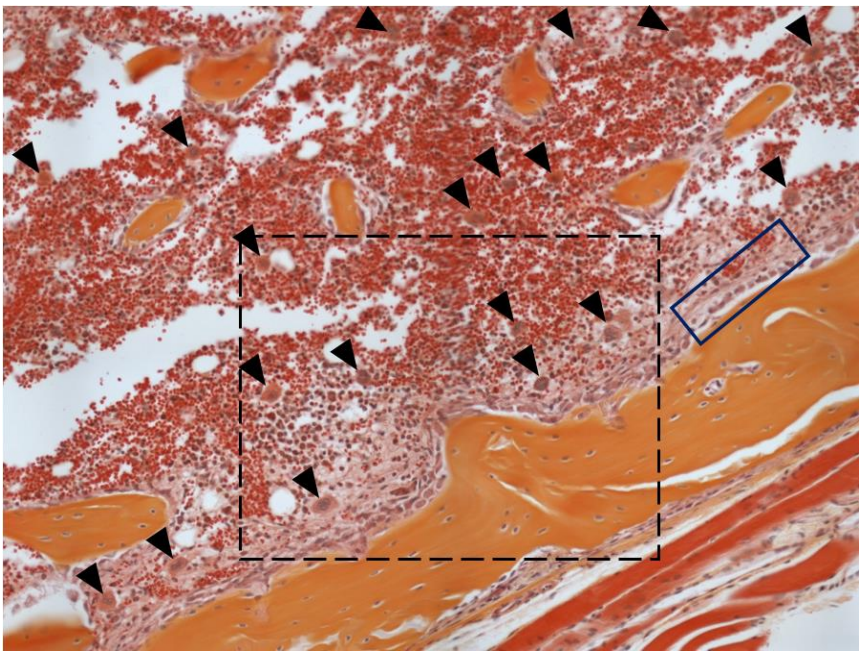

B

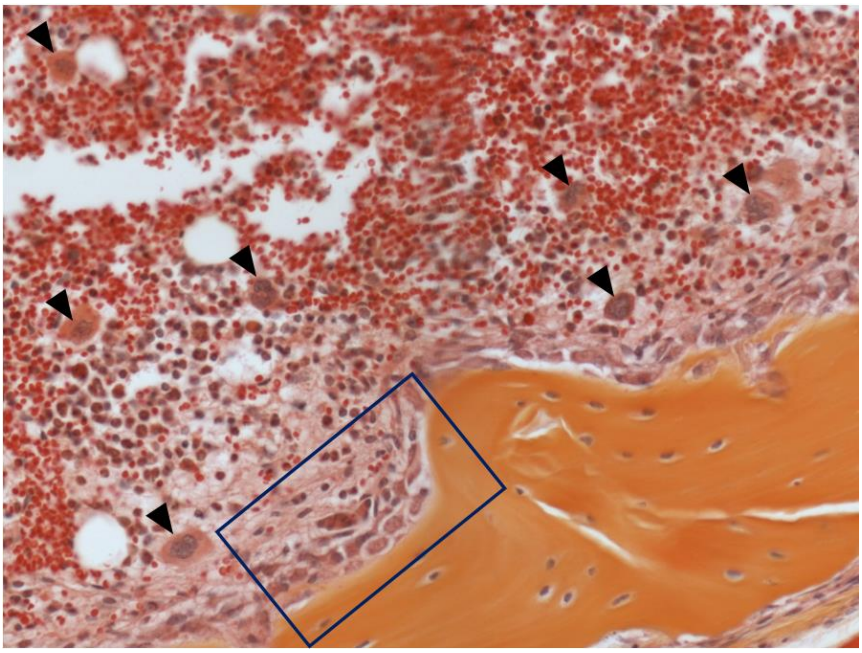

Figure 11. Representative Images from an Irradiated, Vehicle-Treated Mouse

A) Mice (n=7) were irradiated at 650 cGy and treated with vehicle at 24 hours post-irradiation. At 48 hours femurs were harvested, fixed, decalcified (two weeks), paraffin-embedded, sectioned, and stained with hemotoxylin and eosin. A representative image shows pathology of an irradiated mouse femur section. MKs (black arrows) are localized to the areas of bone and even appear to be migrating toward the endosteum. OBs are found in a double to triple layer along the endosteum (blue box). The dashed lines indicate which region of this section has been magnified in 11B.

B) A representative femur section from an irradiated, vehicle-treated mouse shown at 200x magnification. MKs (black arrows) are found in close association with OBs and the bone surface. Note the double to triple layer of OBs along the endosteum (blue box).

Figure 12

A

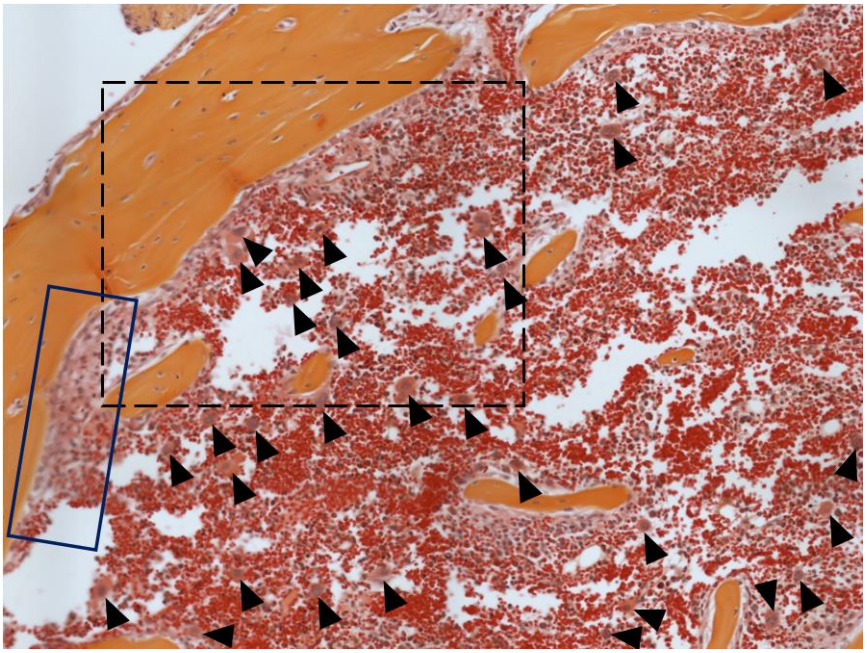

B

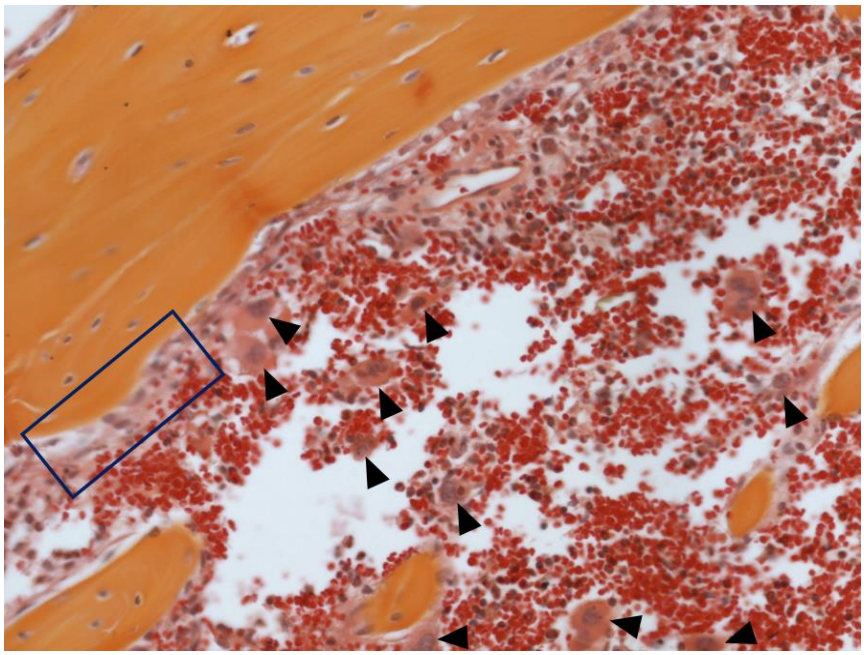

Figure 12. Representative Images from an Irradiated, dmPGE$_2$-Treated Mouse

A) Mice (n=9) were irradiated at 650 cGy and treated with dmPGE$_2$ at 24 hours post-irradiation. At 48 hours femurs were harvested, fixed, decalcified (two weeks), paraffin-embedded, sectioned, and stained with hemotoxylin and eosin. A representative image shows pathology of an irradiated, dmPGE$_2$-treated mouse femur section. MKs (black arrows) are localized to the areas of bone and appear in close association with the endosteum. OBs are found in a double to triple layer along the endosteum (blue box). The dashed lines indicate which region of this section has been magnified in 12B.

B) A representative femur section from an irradiated, dmPGE$_2$-treated mouse shown at 200x magnification. MKs (black arrows) are found in close association with OBs and the bone surface. Note the double to triple layer of OBs along the endosteum (blue box).

Figure 13

A

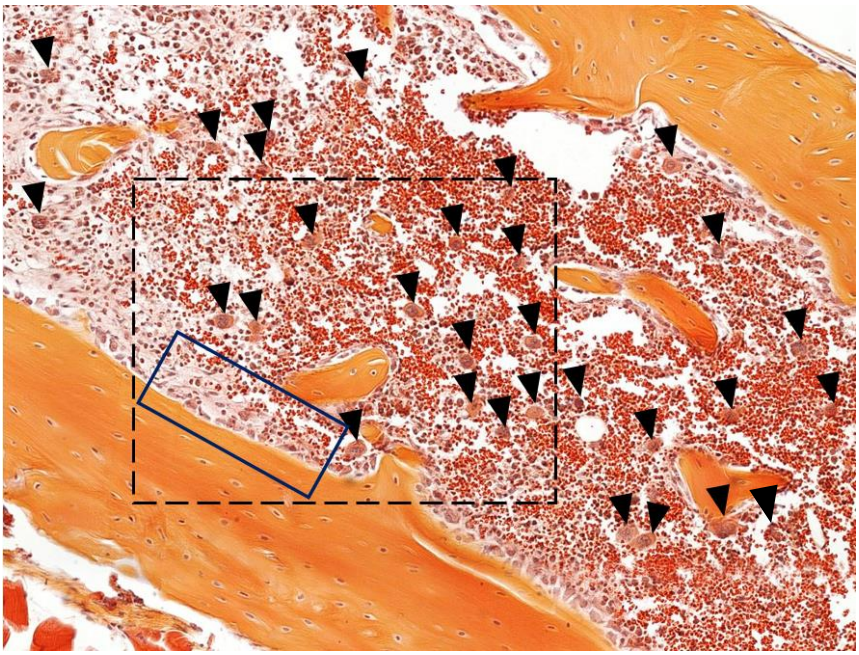

B

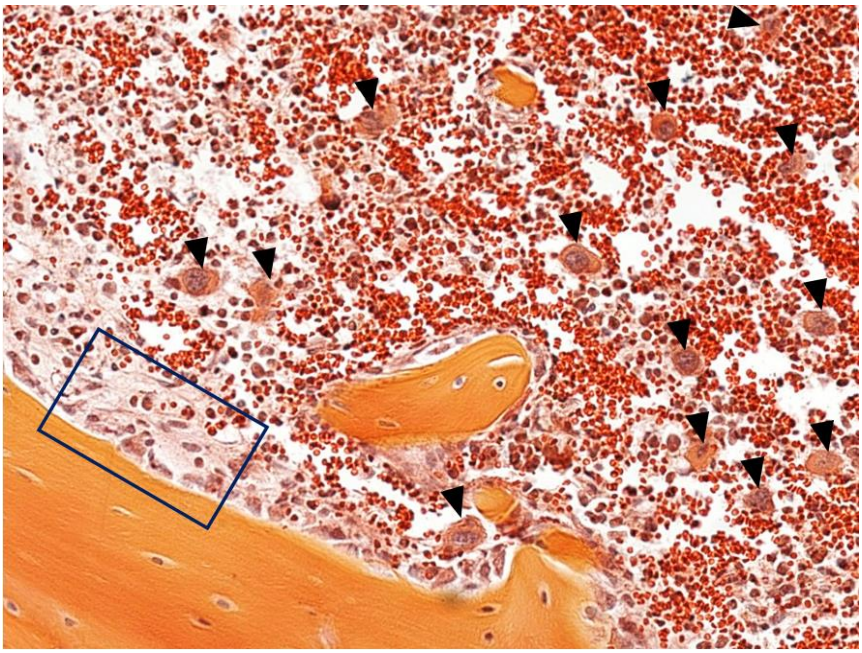

Figure 13. Representative Images from an Irradiated, NSAID-Treated Mouse

A) Mice (n=9) were irradiated at 650 cGy and treated with the NSAID Meloxicam (6 mg/kg) immediately following irradiation and again at 24 hours post-irradiation. At 48 hours femurs were harvested, fixed, decalcified (two weeks), paraffin-embedded, sectioned, and stained with hemotoxylin and eosin. A representative image shows pathology of an irradiated, NSAID-treated mouse femur section. MKs (black arrows) are distributed throughout the bone marrow and some appear to be localized to areas of bone. OBs are found in a double to triple layer along the endosteum (blue box). The dashed lines indicate which region of this section has been magnified in 13B.

B) A representative femur section from an irradiated, NSAID-treated mouse shown at 200x magnification. MKs (black arrows) are distributed throughout the bone marrow with one MK in close association with OBs at the bone surface. There remains a double to triple layer of OBs along the endosteum (blue box).

The total number of MKs and their distance to the endosteum of cortical bone were quantified for each group (n=7-9 mice/group). Total MK number per mm of bone surface did not differ across groups (Figure 14A), suggesting that any changes in MK localization are not a product of proliferation. Approximately 2-fold more MKs were found within 40 μM of the endosteum in irradiated mice treated with vehicle compared to non-irradiated control mice, consistent with data reported by Dominici *et al.* (2009). In mice treated with $dmPGE_2$, this effect was significantly enhanced by an additional 2-fold compared to irradiated mice treated with vehicle (Figure 14B). However, when mice were treated with NSAID, enhancement of MKs within 40 μM of the endosteum was not observed. In fact, levels of MKs within 40 μM of the endosteum were significantly lower than vehicle control suggesting a role for endogenous PGE_2 post-irradiation in migration of MKs to the endosteum. When MKs within 100μm of the endosteum were quantified, the differences between vehicle and $dmPGE_2$-treated mice were lost, but remained significantly higher than in non-irradiated control and NSAID-treated mice (Figure 14C).

Figure 14

A

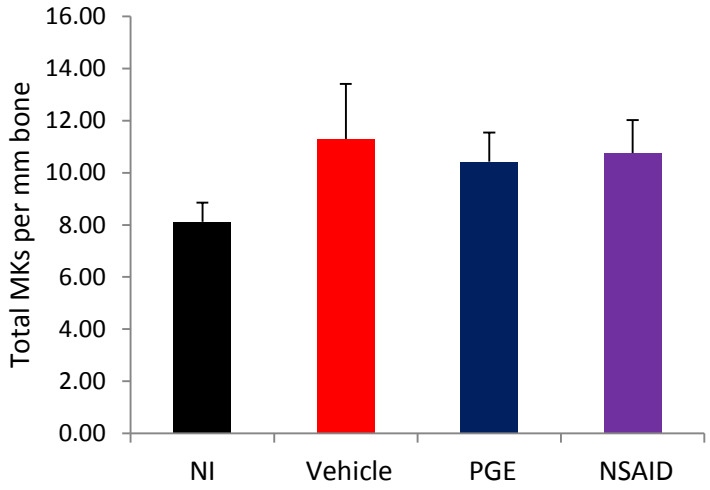

B

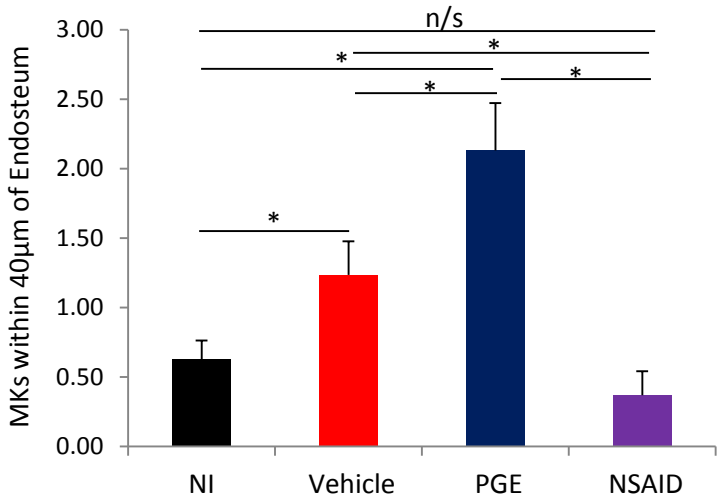

C

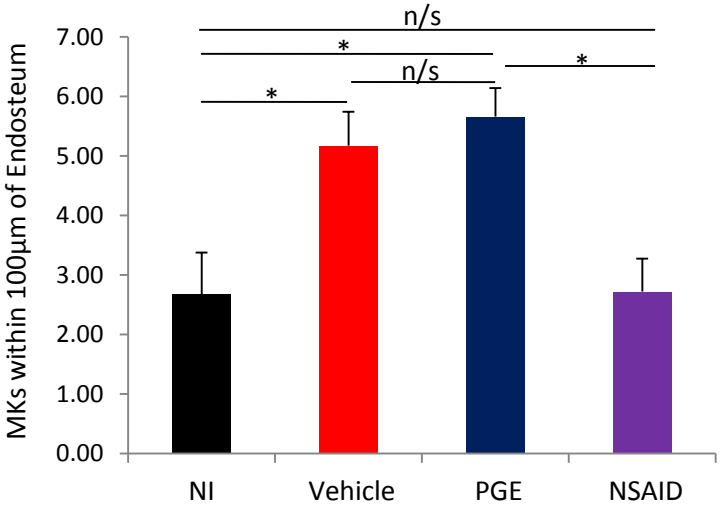

Figure 14. PGE_2 Signaling Increases MK Migration to the Endosteum Post-Irradiation

A) Cohorts of mice (n=7-9 mice per group) were irradiated at 650 cGy and treated 24 hours post-irradiation with vehicle, $dmPGE_2$ (35 μg per mouse), or NSAID (6 mg/kg). Histological analysis reveals no difference in total MK number per mm of bone across treatment groups. Data are mean ± SEM, analyzed by Student's t-test.

B) There is a greater number of MKs within 40μm of the endosteum in irradiated mice treated with vehicle or $dmPGE_2$ compared to non-irradiated control mice or irradiated mice treated with NSAID. Exogenous treatment with $dmPGE_2$ further increases the number of MKs that are found within 40 μM of the endosteal layer. Treatment with NSAID reduces the number of MK within 40 μm of the endosteum down to the same level as seen in non-irradiated control mice. Data are mean ± SEM, analyzed by Student's t-test; * = $p < 0.05$.

C) Quantification of the number of MKs per mm of bone found within 100μm of the endosteum demonstrates increases in MK number in irradiated mice treated with vehicle or $dmPGE_2$ compared to non-irradiated control mice or irradiated mice treated with NSAID. Data are mean ± SEM, analyzed by Student's t-test; * = $p < 0.05$.

Treatment with dmPGE$_2$ Increases MK CXCR4 Expression and Migration to SDF-1

Histological analysis suggests that PGE$_2$ plays an important role in MK migration to the endosteum following radiation exposure *in vivo*. It is well documented that PGE$_2$ increases HSPC migration to SDF-1 via up regulation of CXCR4 (North *et al.*, 2007; Hoggatt *et al.*, 2009), but it remains unknown if MKs respond to PGE$_2$ in a similar way.

In order to investigate the ability of MKs to respond to PGE$_2$ via up regulation of CXCR4, mice were injected with either vehicle or dmPGE$_2$ (35 µg/mouse) and bone marrow cells were collected 24 hours after treatment. Analysis of CXCR4 expression on Lin$^-$CD41$^+$ cells suggests that MKs respond to treatment with dmPGE$_2$ *in vivo* by increasing expression of CXCR4 (Figure 15A). To confirm this finding and translate CXCR4 upregulation to a functional increase in migration, MKs from bone marrow were expanded in culture and migration to 100 ng/mL SDF-1 assayed in a transwell system, following *in vitro* treatment with vehicle or dmPGE$_2$. Migration to SDF-1 increased two-fold when cells were pulse-incubated with dmPGE$_2$ (Figure 15B) compared to vehicle control, suggesting a functional increase in MK migration ($p<0.05$).

Figure 15

A

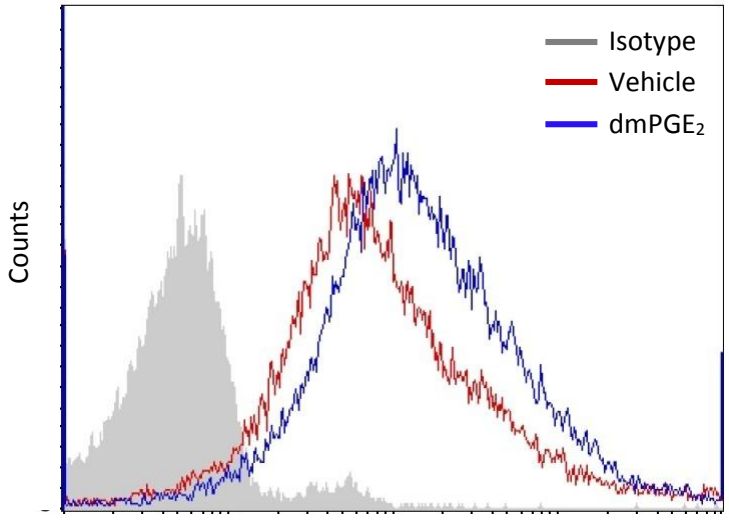
Isotype
Vehicle
dmPGE2
Counts

B

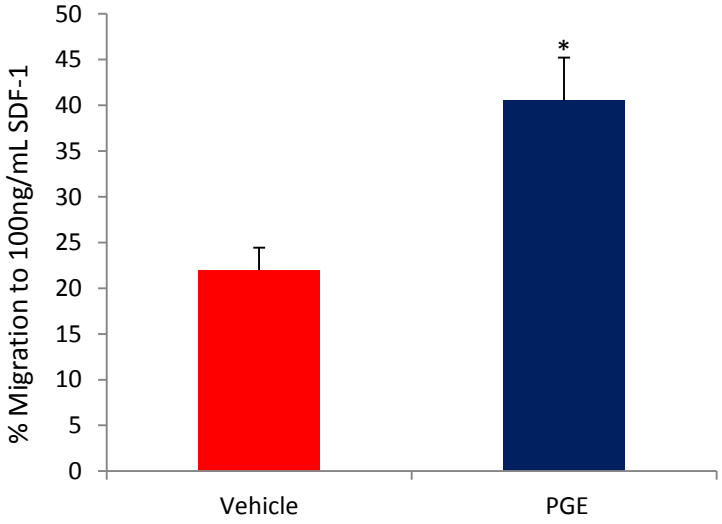
% Migration to 100ng/mL SDF-1
50
45
40
35
30
25
20
15
10
5
0
*
Vehicle
PGE

Figure 15. dmPGE$_2$ Increases MK CXCR4 Expression and Migration to SDF-1

A) Mice (n=3 per group) were injected subcutaneously with either vehicle or dmPGE$_2$. Bone marrow cells were collected 24 hours after treatment, lineage depleted and analyzed via flow cytometry for expression of CXCR4. Lin$^-$ CD41$^+$ MKs showed increased expression of CXCR4 with dmPGE$_2$ treatment.

B) MKs were cultured and expanded *in vitro* for 7 days. Following expansion, cells were treated with either vehicle or dmPGE$_2$ and allowed to migrate to 100 ng/mL SDF-1 in a transwell system. Migration of MKs (Lin$^-$ CD41$^+$ cells) increased two-fold with dmPGE$_2$ treatment. Data are mean ± SEM, analyzed by Student's t-test; * = $p < 0.05$.

Discussion:

Our data indicate a critical role for PGE_2 signaling in MK migration to the endosteum of cortical bone following sublethal irradiation. An increased number of MKs were found localized to the endosteum in irradiated mice treated with vehicle and an even greater number were seen in irradiated mice treated with $dmPGE_2$, with no change in total MK number across all groups. This effect was lost when endogenous PGE_2 signaling was blocked via NSAID administration. Taken together, the data reveal that PGE_2 signaling is required for MK migration to the endosteum after irradiation, and exogenous administration with $dmPGE_2$ further enhances MK migration.

A recent study by Olson *et al.* (2013) supports these results showing that MKs are recruited to the endosteal layer after lethal irradiation. Furthermore, they demonstrate that migration of MKs to the endosteum is required for OB expansion and expansion of the HSC niche. Suppression of TPO signaling through the MK receptor cMpl and blockade of MK-derived PDGF-BB signaling was shown to prevent expansion of OBs. In our studies, administration of NSAID did not abrogate OB expansion at 48 hours post-irradiation but MK migration to the endosteum was lost. *In vitro* data suggest that $dmPGE_2$ increases MK expression of CXCR4 and migration to SDF-1. As a result, PGE_2 signaling appears to be crucial for MK upregulation of CXCR4 and subsequent recruitment to the endosteum, but not for expansion of OBs. Future studies are planned to evaluate if OB proliferation/differentiation differs between irradiated mice treated with vehicle, $dmPGE_2$, or NSAID. A specific population of immature OBs has been shown to facilitate HSC maintenance, while co-culture with more mature OBs results in loss of

HSC repopulating ability (Chitteti *et al.*, 2010; Chittetti *et al.*, 2013). Therefore, we hypothesize that MK migration and subsequent stimulation of OBs skews OB proliferation/differentiation toward hematopoietic support (immature OBs) at the expense of bone formation (mature OBs).

Olson *et al.* (2013) also demonstrated that MK recruitment to the endosteum is required for engraftment of donor HSC in a transplant scenario. MKs facilitate recovery of the HSC niche and blockade of MK recruitment resulted in graft failure. Based on our results, HSC transplantation may be improved by administration of PGE_2 to the recipient. Exogenous supplementation with $dmPGE_2$ should enhance the migration of MK to the endosteum to promote recovery of the endosteal niche and facilitate higher donor cell engraftment.

Past studies have revealed a relatively radioresistant population of MKs within human bone marrow (Gruzdev *et al.*, 1996) and umbilical cord blood (Kashiwakura *et al.*, 2000; Kashiwakura *et al.*, 2005). Mature MKs appear to be radioresistant and maintain their platelet-producing capabilities after exposure to radiation, even at very high doses. Due to the radioresistant nature of MKs, it is not likely that an effect on MK survival would be noticeable at only 48 hours post-irradiation. Therefore, it is impossible to determine from these experiments if irradiation and subsequent treatment with vehicle, $dmPGE_2$, or NSAID has an effect on long-term survival of MK populations.

Chapter 4. Future Directions

Evaluating the Effect of dmPGE$_2$-Treatment Post-Irradiation on the HSPC

Our data demonstrate the ability of dmPGE$_2$ to act as an effective radiomitigative agent in both lethally and sublethally-irradiated mice. Current data suggest that, although PGE$_2$ is known to promote HSPC survival through upregulation of Survivin (Hoggatt *et al.*, 2009), dmPGE$_2$-treatment post-irradiation does not increase Survivin levels at early time points. We plan to validate these data by extending our time-course study to include earlier and more frequent time points, i.e. 6 hours after treatment at 6 hour intervals, and by analysis of Survivin mRNA levels by RT-PCR. Based on other known effects of PGE$_2$ on the HSPC, we also propose to evaluate cell cycle and proliferation in LSK and SLAM-LSK populations in additional time-course studies. PGE$_2$ increases HSC entry into and progression through cell cycle (Hoggatt *et al.*, 2009), which may play an important role in its effects as a radiomitigative agent.

Analysis of the radiomitigative effects of PGE$_2$ on the HSPC populations will also include investigation into which EP receptor is responsible for PGE$_2$ signaling. As previously discussed, PGE$_2$ signals through four different receptors (EP1-EP4) that are all expressed on HSPCs. Our laboratory has access to germ line receptor knock-out mice for receptors EP1-EP3 and have created a Tamoxifen-Cre inducible knock-out of EP4. Using these mice we will evaluate the radiomitigative effects of dmPGE$_2$ in chimeric mice composed of bone marrow cell knock-outs transplanted into lethally irradiated recipients. In this scenario, each group of knock-out mice will have HSPCs lacking a

specific EP receptor but the bone marrow microenvironment will remain wild type. This will allow us to evaluate the loss of each specific EP receptor on the ability of PGE_2 to successfully mitigate the effects of irradiation.

We also wish to evaluate the effect of $dmPGE_2$-treatment post-irradiation on induction of DNA repair mechanisms. Ionizing radiation produces DNA double-strand breaks (DSB) that are recognized by the phosphorylated-H2AX protein (γ-H2AX) (Balajee and Geard, 2004; Kuo and Yang, 2008). γ-H2AX molecules accumulate at sites of DNA DSB, producing nuclear foci and facilitating initiation of DNA repair. Under normal conditions in mammalian cells, accumulation of γ-H2AX foci at sites of DNA damage occurs rapidly and then disperses within 1-3 hours as the majority of DNA is repaired. We will use the Imagestream Mark II instrument (Amnis, Seattle, WA) to visualize the DNA repair process in irradiated bone marrow cells collected from vehicle and $dmPGE_2$-treated mice. If PGE_2 is able to promote or induce the DNA repair process, we expect to see faster initiation of repair mechanisms and repair completion; γ-H2AX foci will accumulate quickly and then rapidly disperse.

Finally, further studies evaluating the survival of LD 70/30 irradiated mice treated with vehicle, $dmPGE_2$, or NSAID will be performed. Bone marrow cells will be collected from surviving mice and secondary and tertiary transplants performed to assess the long-term repopulating capability of HSPC within these mice and ensure they are not prone to abnormal pathology, such as bone marrow failure or leukemia.

Evaluating the Effect of dmPGE$_2$-Treatment Post-Irradiation on the Endosteal Niche

The role of OBs in hematopoietic support has been well explored. As early as the 1970s, it was determined that HSCs are found in close proximity with endosteal surfaces of bone (Lord and Hendry, 1972; Lord *et al.*, 1975). Both human and murine OBs have been shown to produce cytokines important for hematopoietic support and maintenance, including G-CSF, GM-CSF, M-CSF, SCF, and SDF-1 (Kacena *et al.*, 2006). More recent studies show that co-cultures of OBs with HSPCs expand their CFU and repopulating potential, which is mediated through Notch signaling (Chitteti *et al.*, 2010). Additionally, cells of the OB niche have been organized into a hierarchy of maturation that reveals the importance of CD166 expression in maintenance of HSC with long-term repopulating capabilities (Chitteti *et al.*, 2013). Immature OBs and MSCs retain expression of CD166 and the ability to support HSCs, while mature OBs do not express CD166 and demonstrate a decreased ability to support hematopoiesis.

Our data demonstrate an increase in OBs along the endosteum of cortical bone after irradiation, but it is unknown whether or not this increase is due to proliferation or differentiation. Using a three-color GFP-reporter mouse (Ushiku *et al.*, 2010), we plan to analyze the proliferation and differentiation state of OBs from irradiated mice treated with vehicle, dmPGE$_2$, or NSAID to elucidate the role of PGE$_2$ in OB proliferation and maturation. Additionally, we will collect osteoblast lineage cells and use flow cytometry and co-culture studies to determine their immunophenotypic profile and ability to support hematopoiesis, respectively. We hypothesize that PGE$_2$-induced MK migration to the endosteum skews osteolineage cell differentiation toward hematopoietic support

at the expense of bone formation. Preliminary analysis of bone volume 30 days after LD 70/30 irradiation demonstrates decreased bone volume in a mouse treated with $dmPGE_2$ at 24 hours post-irradiation compared to a mouse treated with vehicle (Figure 16). Further experiments will investigate the hypothesis that exogenous PGE_2 administered post-irradiation facilitates recovery of hematopoiesis at the expense of bone.

Our results indicate that PGE_2 signaling is required for MK recruitment to the endosteum post-irradiation, and this effect can be enhanced with exogenous administration of $dmPGE_2$. The effect of $dmPGE_2$-treatment on the MK appears to be through upregulation of CXCR4 and, consequently, increased migration to SDF-1. In order to confirm this, we will administer AMD3100 (a CXCR4 antagonist) and evaluate its effects on MK migration via histology; we propose that AMD3100 will have a similar effect as NSAID administration.

In order to further investigate the role of the MK on niche restoration after irradiation, we will evaluate MK survival in a time-course study. Femurs from lethally irradiated mice will be analyzed histologically over a period of time up to 30 days post-irradiation. This will allow us to determine if $dmPGE_2$ treatment post-irradiation is also having an effect on MK survival and, therefore, enhancing HSPC recovery.

We will also examine if PGE_2 is acting directly on the MK and which EP receptor is responsible. We have recently obtained a mouse expressing Cre-recombinase under the platelet factor 4 (PF4) promoter which is MK-specific (Jackson Laboratory; Bar Harbor, ME). Crossing this mouse with our EP4-flox and, separately, our CXCR4-flox mice will

generate MK-specific EP4 and MK-specific CXCR4 knock-out mice. Radiation studies and analysis of MK migration and hematopoietic recovery in these mice will allow us to investigate the role of the EP4 receptor and CXCR4 in the radiomitigative effect of dmPGE$_2$.

Figure 16

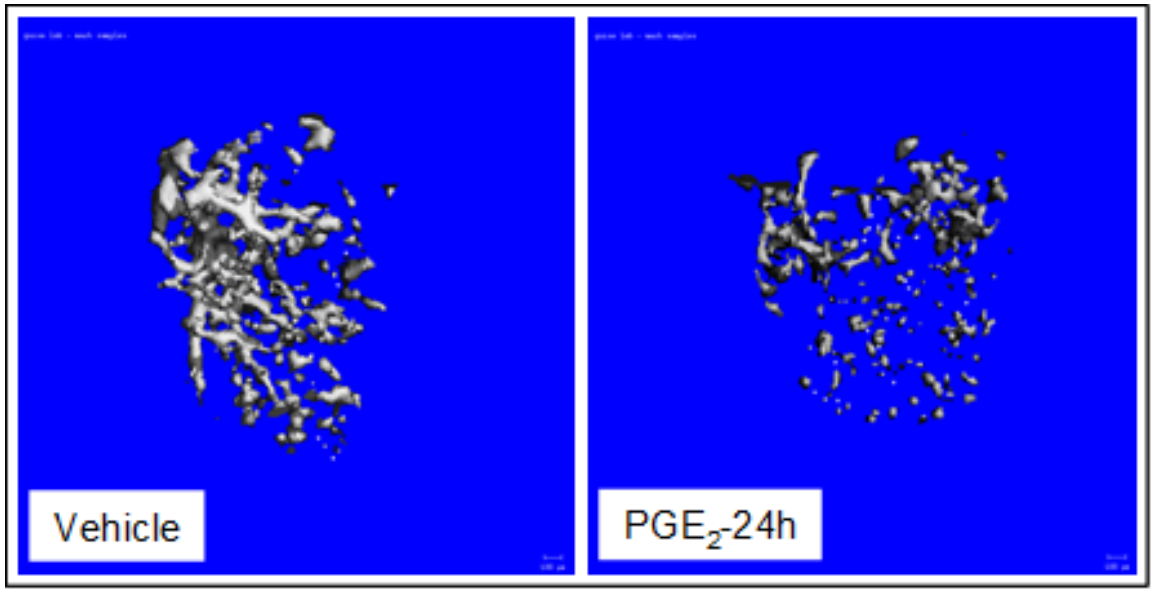

Figure 16. dmPGE$_2$-Treatment Post-Irradiation Decreases Bone Volume

Micro-CT analysis at 30 days post-LD 70/30 irradiation of mice treated 24 hours after irradiation with vehicle or dmPGE$_2$. Treatment with dmPGE$_2$ leads to decreased bone volume compared to vehicle control, suggesting that PGE$_2$ may facilitate hematopoietic recovery at the expense of bone formation.

Evaluating the Effect of dmPGE$_2$-Treatment Post-Irradiation on the Endothelial Niche

PGE$_2$ is known to promote angiogenesis (Zhang and Daaka, 2011) and endothelial cell migration (Rao *et al.*, 2007) and survival (Kamiyama *et al.*, 2006; Dada *et al.*, 2008). Similar to the studies proposed to examine the endosteal niche, we would like to evaluate the effects of PGE$_2$ as a radiomitgator on the endothelial niche. Treatment with dmPGE$_2$ post-irradiation may increase endothelial cell survival and/or promote migration of endothelial cells to the damaged areas of the bone marrow. Assays for endothelial cell migration, proliferation, and survival (Survivin expression and markers of apoptosis) will evaluate the potential effects of dmPGE$_2$ on this cell population. Additionally, if an effect on the endothelial cell is noted, we will determine which receptor is responsible for the effect.

Translation to the Clinic

The development of PGE$_2$ as a radiomitigative agent that promotes hematopoietic recovery and HSC niche restoration has the potential to significantly affect treatment following a radiation accident or to improve the bone marrow transplant process. In the case of a radiation accident, an ideal radiomitigator is safe and effective regardless of radiation exposure, age, or health status, is easily administered, and allows for rapid distribution. Once the mechanism of action for dmPGE$_2$ to facilitate hematopoietic recovery is defined and understood, it may be possible to selectively target the receptor responsible via specific receptor agonists. Agonists for all EP receptors are commercially available and may be even more effective than dmPGE$_2$.

In a transplant scenario, $dmPGE_2$ treatment may promote restoration of the HSC niche after radioablation and increase engraftment and transplant efficiency. Additional studies will be performed using limiting dilutions of donor cells with competitors into recipient mice that have been treated with vehicle, $dmPGE_2$, or NSAID. Analysis of recipient mice survival, engraftment, and long-term repopulating capability via secondary transplant will determine if $dmPGE_2$ treatment of the recipient has the ability to enhance transplantation efficiency. These studies will be extended to evaluation of HSC niche restoration following chemotherapy using 5-fluorouracil (5-FU). We will investigate the ability of mice treated with either vehicle or $dmPGE_2$ to recover from and undergo subsequent rounds of 5-FU treatment. Treatment with $dmPGE_2$ may enhance niche restoration and allow mice to recover from chemotherapy more quickly and increase tolerance to additional therapy.